Journal of Cleaner Production 413 (2023) 137403

Contents lists available at ScienceDirect

Journal of Cleaner Production

journal homepage: www.elsevier.com/locate/jclepro

Designing globalized robust supply chain network for sustainable biomass-based power generation problem

Aixia Chen [a], Yankui Liu [b,*]

[a] School of Management, Hebei University, Baoding 071002, Hebei, China

[b] Hebei Key Laboratory of Machine Learning and Computational Intelligence, College of Mathematics & Information Science, Hebei University, Baoding 071002, Hebei, China

ARTICLE INFO

Handling Editor: Cecilia Maria Villas Bôas de Almeida

Keywords:
Power generation supply chain
Sustainability
Uncertainty set
Globalized robust optimization
Goal programming

ABSTRACT

The utilization of renewable energy sources to produce electricity is capable of relieving the pressure of limited natural resources and achieving the sustainability of future energy. This paper addresses a multi-period multi-feedstock multi-technology biomass-based power generation supply chain planning problem with parameter uncertainty, balancing economic, environmental, and social objectives simultaneously. However, the main challenges in optimizing this problem are correlated with multiple conflicting objectives and uncertain parameters. This study proposes a novel globalized robust goal programming model with goal constraints to balance three conflicting objectives using priority levels and characterize the uncertainty of unit emissions and social scores by inner–outer uncertainty sets. After transforming globalized robust environmental and social goal constraints into their equivalent forms, the tractable counterpart of the proposed model is obtained, which is mixed-integer linear programming (MILP). Finally, the effectiveness of the proposed model is demonstrated through a case study about the design of a sustainable biomass-based power generation supply chain (SBPSC) network in Hubei Province, China. Computational results reveal that by adjusting several parameters, environmental and social aspired goals consistently can achieve, whereas the economic objective is vulnerable to being influenced. Comparative studies with nominal goal programming model and robust goal programming model indicate that the proposed model is uncertainty-immunized and less conservative. Under investigated circumstances, the realized economic profit by the proposed model is approximately 42.5% higher than that of the robust goal programming model on average.

1. Introduction

The growth of population, changes in lifestyle, and the improvement of people's living standards have collectively resulted in a significant increase in global energy demand through decades, particularly in industrialized countries. According to BP (2022), primary energy consumption grew by 5.8% in 2021, exceeding the levels reported in 2019 by 1.3%, whilst oil demand rose by 5.3 million barrels per day, natural gas demand increased by 5.3%, and coal demand increased by more than 6%, which is a little higher than the levels observed in 2019 and represents the highest point since 2014. Given the prevailing trend, it is evident that non-renewable sources of energy cannot single-handedly cope with the mounting pressure, thereby highlighting the requirement for alternative energy sources to supplement energy demands (Cambero and Sowlati, 2014). Intergovernmental Panel on Climate Change asserts a reality that global warming is caused by greenhouse gas emission, which primarily results from the utilization of fossil energy (Intergovernmental Panel on Climate Change, 2018). To assure future energy sustainability and address the environmental issues with global warming, several countries are now turning to renewable sources for their energy production needs.

The renewable electricity sector has grown rapidly over the years with an annual growth rate of approximately 5% from 2000 to 2019 (Global Bioenergy Statistics, 2021). In 2019, the power produced from renewable energy was 7311 TWh, where hydro, wind, and biomass, respectively, were ranked the first, second, and third largest renewable power generation sources (See Fig. 1). Hydropower is a power generation technology that is both clean and efficient, while also being hassle-free; however, the initial cost is very high and can potentially lead to serious environmental consequences, such as flood, water pollution, and damage to marine life (Singh and Singal, 2017). Wind energy is clean, low cost, and environmentally friendly; however, its fluctuating output caused by wind direction, temperature, pressure, and humidity poses a significant challenge (Mittal et al., 2016). Biomass is

* Corresponding author.
E-mail addresses: chenaixia@hbu.edu.cn (A. Chen), yliu@hbu.edu.cn (Y. Liu).

https://doi.org/10.1016/j.jclepro.2023.137403
Received 18 January 2023; Received in revised form 30 April 2023; Accepted 5 May 2023
Available online 10 May 2023

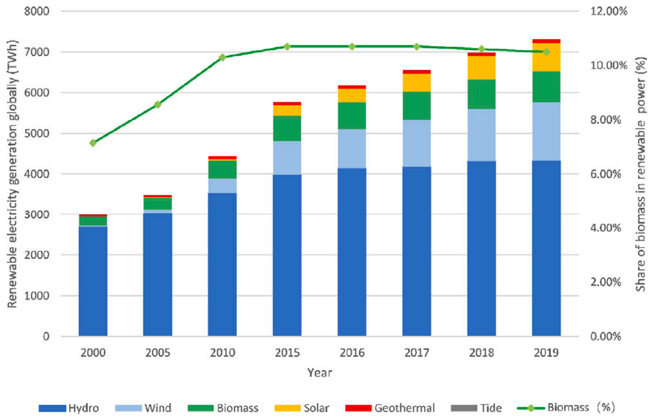

Fig. 1. Renewable electricity generation in 2000–2019.

globally available due to the diverse range of sources it encompasses, including agricultural and forest residues, energy crops, animal fats, municipal wastes (Miret et al., 2016). In addition, biomass energy possesses a distinctive superiority over other renewable energy sources as it can be transported, stored, and utilized in locations away from its source (Simon et al., 2021). Furthermore, biomass energy production offers new sources of income for farmers and helps to reduce landfill waste (Tillman, 2000). Despite these benefits, the utilization of biomass energy still presents certain challenges, including low energy density, low calorific value, and high logistic costs (Cambero and Sowlati, 2014).

Based on the characteristics of biomass energy, first-generation biomass typically refers to crops like corn and sugarcane that compete with the food industry (Hombach et al., 2016). For alleviating the situation, second-generation biomass is receiving increasing development, which primarily involves perennial grasses, organic residues, and wastes (Miret et al., 2016). These sources generate less greenhouse gas emissions, and the environmental impact of waste disposal can be reduced when organic residues and wastes are utilized for production (Miret et al., 2016). In China, the Work Plan for the Construction of Biomass Power Generation Projects in 2021 was issued to promote the steady and healthy development of agricultural and forestry biomass and waste power generation industries. Data from the National Energy Administration reveal that in 2021, China produced 8.08 million kWh of biomass power generation. In this study, given that forestry, agriculture, and animal husbandry are among the most significant economic activities in Hubei, China, second-generation biomass, particularly forestry and agricultural residues and animal waste, are taken into account as potential feedstocks for power generation.

The challenge of low energy density and high logistic costs of biomass energy requires the development of transportation plans and storage settings for biomass production (Ahmadvand and Sowlati, 2022). To optimize the biomass power generation system, various decisions must be taken, such as biomass purchasing quantities, transportation quantities, inventory level, the location of storage facilities, and power generation technology selection, which highlights the importance of overall system planning (Zandi Atashbar et al., 2018). In general, the overall system diagram of optimizing biomass power generation supply chain is displayed in Fig. 2. Several studies (e.g., Evans et al., 2010; Ruiz et al., 2013) have explored the performances of different power generation technologies on the economic objective, environmental damage, and social impact. Furthermore, Yang et al. (2020) studied the importance of environmental-social-economic dimensions to sustainable development from the perspective of footprint calculation. Hence, a biomass-based power generation system that simultaneously considers environmental, social, and economic objectives should be investigated for sustainable planning. However, there are several uncertainties caused by limited historical data availability, such as unit emissions and social scores, which complicate the sustainable biomass power generation system.

When designing the SBPSC network, the unit emissions of harmful substances cannot be accurately determined by the influence of biomass quality and power generation environment amongst others. Similarly, the scores of each power generation technology on a certain social factor are difficult to obtain precisely owing to epistemic uncertainty and measurement errors. These uncertainties are closely associated with environmental and social objectives and therefore should be considered in sustainable biomass power generation systems. The above discussions raise the following questions that need to be addressed:

(1) What type of uncertainty-immunized optimization model should be developed for this sustainable biomass-based power generation system considering environmental-social-economic dimensions?

(2) How does the setting of environmental and social goals impact the achievement of economic goal?

(3) What are the advantages of our proposed model in terms of achieving the three conflicting goals?

To address these questions, the first task is to characterize the uncertain parameters. Given the limited data available, only a general value range of uncertain parameters can be acquired. This situation suggests globalized robust optimization (GRO) method (Ben-Tal et al., 2017), which extends the robust optimization method (Ben-Tal et al., 2009). The motivation for using the GRO method is that the optimal solution obtained by GRO method can not only hedge against multiple uncertainties, can also be less conservative. The second task involves solving a multi-objective problem in which the desired environmental, social, and economic goals are known in advance, according to quotas and requirements of the environmental protection and human resources departments, as well as the power plant's development. The realization of each goal has varying degrees of importance for the decision-maker, leading to the selection of the goal programming method to prioritize and achieve the objectives (Charnes and Cooper, 1961).

Thus, this study proposes a novel globalized robust goal programming method to handle parameter uncertainties and prioritize environmental, social, and economic objectives. Specifically, the main contributions are as follows:

- We study the SBPSC network design problem and propose a new globalized robust goal programming model from a different optimization perspective. Distinct from relevant literature, this study incorporates the parameter uncertainty and the preference of decision-makers into the proposed model, which are characterized by the uncertainty set and priority level, respectively.
- We derive a tractable counterpart form of the proposed globalized robust goal programming SBPSC model with goal constraints, which is a MILP model. By introducing the inner–outer uncertainty set to describe the uncertain unit emissions and social scores, this study formulated the globalized robust environmental and social goal constraints and then transformed them into equivalent forms.
- We demonstrate the effectiveness of the proposed model through a case study of the SBPSC network design problem. The results indicate that environmental and social goals can always be achieved, whilst the economic goal is susceptible to the variation of parameters. Compared to the nominal and robust goal programming models, the proposed model is not only uncertainty-immunized but also less conservative.

The rest of this paper is organized as follows. Section 2 reviews the related literature. Section 3 states the studied SBPSC problem. Section 4 proposes a globalized robust goal programming SBPSC model. Section 5 presents the derivation of the tractable counterpart form of the proposed model. In Section 6, a case study is narrated. Section 7 reported the numerical and managerial results, and Section 8 concludes the study.

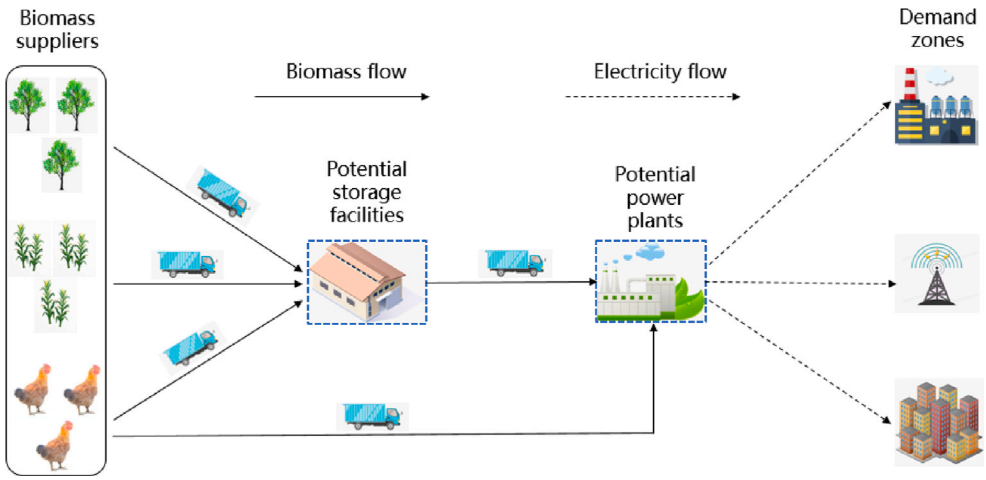

Fig. 2. Overall diagram of biomass-based power generation supply chain.

2. Literature review

This section reviews the related literature about biomass supply chain from the following aspects: the considerations of environmental and social impacts, the network designs and uncertain optimizations of the mentioned supply chain, and then highlights the identified research gap.

2.1. Considerations of environmental and social impacts

Lake et al. (2015) proposed a standardized instrument, i.e., life cycle assessment (LCA) approach, to calculate the environmental effects of products from inception to final disposal. The LCA approach has been employed in various research fields (e.g. Acquaye et al., 2017; Smith et al., 2018; Mena and Schoenherr, 2020) to reduce negative impact on the environment and create a green system. Only a limited number of studies (e.g. Fattahi et al., 2021) have considered the impact of not only greenhouse gas emissions but also air pollutants and toxic emissions on the environmental performance in supply chain network design. This research differs from most existing literature by evaluating the environmental impact of biomass-based power generation supply chains regarding not only CO_2 emissions but also hazardous emissions and air pollutants.

Evans et al. (2010) evaluated the wide societal implications of power generation technology and biomass types derived from biomass energy production. Following that, some articles (e.g. Almeida et al., 2013; Barbosa-Póvoa et al., 2018) assessed several social factors usually addressed in the supply chain network design problems, such as job creation, social approval and annual turnover. To determine the social impact of goods and create a framework for addressing critical social indicators, Andrews (2009) developed a well-known methodology Social Life Cycle Assessment (S-LCA), which has been applied in the bioenergy supply chain problem (Fattahi et al., 2021; Habib et al., 2020). Unlike most existing literature, the social impact of biomass supply chains is identified through annual turnover, worker harm, job creation, and social acceptance in this paper.

2.2. Biomass supply chain network design

The biomass supply chain planning and network design is currently popular among academics and practitioners owing to the utilization of biomass to produce bioenergy in some countries. Traditionally, proposed models for optimizing biomass supply chains focused on the economic objective in literature. For instance, Mirhashemi et al. (2018) formulated a MILP model based on these locations selected through the CWDEA approach to optimize the M.oleifera-based biodiesel supply chain network design problem. Wu et al. (2022) presented a MILP model that aims to decrease feedstock supply costs and minimize the total cost by utilizing economies of scale in biomass supply chain networks. In contrast, Kwon et al. (2022) proposed a multi-period MILP model that takes long-term variations of waste usage and biodiesel demand into account, with the objective of minimizing the average annual cost of the whole supply chain network. A long-term design of renewable fuel supply chains was studied by Wolff et al. (2023), and the seasonal availability of various biomass resources was considered in the proposed mathematical model. Tesfamichael et al. (2021) developed an optimization model that aims to minimize the investment cost and maximize the profit to solve the problem of high initial investment costs and less economic attractiveness of the biomass-to-biofuel supply chain.

With the impact of global warming becoming more apparent, environmental issues related to carbon emissions from biomass supply chains are receiving increasing attention. Rahmani Mokarrari et al. (2023) investigated the techno-economic feasibility of building a biofuel production facility and discovered that only taking the impacts of GHG emission reduction into account makes biofuel production economically feasible. Considering carbon emissions and time-dependent market quotas, Hombach et al. (2016) presented a MILP model to optimize the second-generation biofuel supply chain with the aim of net present value maximization. Fernández-Puratich et al. (2021) presented a bi-objective optimization model that minimizes total cost and carbon emissions to access the economic and environmental values of different kinds of biomass for power production and heating. To minimize the total cost and GHG emissions of the biomass-to-electricity supply chain, Nandimandalam et al. (2022) developed a multi-objective mathematical model to determine power plant locations, biomass supplier allocations, and other various decisions. García-Velásquez et al. (2022) proposed a bi-objective optimization model that considers economic and environmental criteria for designing biobased supply chain networks. Several studies have aimed to optimize sustainable biomass supply chains by minimizing total cost while considering environmental impacts as a constraint (e.g. Basile et al., 2022).

There is limited literature incorporating social impacts in the sustainable biomass supply chain network design to the best of the authors' knowledge. Considering the economic, environmental, and social dimensions of the sustainable development, Miret et al. (2016) formulated a MILP model to design a green bioethanol supply chain, in which the social aspect is evaluated by the overall number of locally increased jobs as well as competition between energy and food. Singh et al. (2022) developed a multi-objective optimization model with the aim of total cost and environmental impact minimization and social impact maximization in planning waste animal fat to biodiesel supply chains. Meanwhile, Cambero and Sowlati (2014) and Sun and Fan

(2020) provided a review of recent research on the evaluation and optimization of biomass supply chains, including modeling techniques, solution methods, and possible research directions for the future.

Uncertainty is one of the main challenges in biomass supply chain planning, as various sources of uncertainties exist due to unpredictable weather patterns, unstable economic conditions, and advancements in biomass power production technologies. However, the studies mentioned earlier have not taken into account these uncertainties.

2.3. Uncertain optimization in biomass supply chain network design

Given the complex network structure and changeable external environment, the biomass supply chain is subject to significant degrees of uncertainties. Previous studies have primarily focused on uncertain parameters, including transportation costs, demand for bioenergy, and biomass feedstock supply in biomass supply chains. To address such uncertainties, stochastic programming, fuzzy programming, and robust optimization have been widely used as effective modeling tools.

Amongst the existing techniques for dealing with uncertainty, stochastic programming is one of the most widely used techniques in optimizing the biomass supply chain. Under the uncertainty of power demand, biomass quality, and availability, Saghaei et al. (2020) proposed a two-stage stochastic programming model with chance constraints to minimize the overall cost. Aim for the profit of bio-energy supply chain maximization, Memisoğlu and Üster (2021) presented a two-stage stochastic programming model considering the uncertainty of biomass yield and price and designed an L-shaped-based algorithm to solve the model efficiently. Aranguren et al. (2021) developed a stochastic hub-and-spoke network model to minimize logistical costs and designed an efficient solution scheme that is achieved by using Simulated Annealing. Guo et al. (2022) proposed a multiperiod stochastic programming model under the uncertainty of corn stover supply and farmer participation rates. Computational results indicate that the stochastic programming model obtains significantly higher cost savings than the deterministic programming model in the validation period.

Some literature integrates environmental or social dimensions into the modeling of biomass supply chains and utilizes stochastic programming to cope with the uncertainty. Díaz-Trujillo et al. (2020) proposed a multi-objective stochastic programming model to explore the effects of uncertain stock availability and biogas demand on the economic and environmental objectives in biomass supply chains. Mohtashami et al. (2021) introduced a multi-objective model aiming at cost minimization, social benefit, and environmental impact maximization. Aranguren and Castillo-Villar (2022) proposed a bi-objective model, which is solved by applying the ϵ-constraint method and metaheuristic method to obtain Pareto frontier approximations. Aboytes-Ojeda et al. (2022) developed a two-stage stochastic optimization model that aims to minimize expected total cost and CVaR simultaneously and is solved using a hybrid method associated with the Simulated Annealing algorithm. To hedge against the risk originating from uncertainties, Díaz-Trujillo et al. (2020), Fattahi et al. (2021), and Khezerlou et al. (2021) also incorporated various risk conceptions caused by multiple uncertainties in the modeling of biomass supply chains.

The applications of simulation methods in designing supply chain networks were reviewed by Tordecilla et al. (2021). Additionally, they grouped the existing approaches according to their methodology, level of uncertainty, and risk factors. Lo et al. (2021) adopted the Monte Carlo simulation method for measuring the techno-economic feasibility of biomass gasification processes under various uncertainties. To analyze biomass supply chains in terms of the environmental and economic performances, Karimi et al. (2021) proposed a bi-objective stochastic optimization model where chance constraints are solved by the sample average approximation method. Simon et al. (2021) estimated the feasibility of technology and operating costs of wood biomass production more precisely by using the simulation approach and indicated the available quantity of woody biomass and the range of extraction costs in simulation results. According to the recursive optimization-simulation approach, Akhtari and Sowlati (2020) combined an optimization model and a simulation model to develop a hybrid model, which can determine strategic and tactical decisions and measure the variations at the operational level at the same time.

Fuzzy or possibility programming is another common technique to handel uncertainty in biomass supply chain optimizing problems, which is usually used to characterize epistemic uncertainty (Habib et al., 2020). For instance, Ghaderi et al. (2018) presented a multi-objective possibility programming model for designing the bioethanol supply chain network under the epistemic uncertainty in the data with the simultaneous considerations of environmental, economic, and social objectives. Habib et al. (2020) optimized a waste-biodiesel supply chain using a modified robust possibilistic chance-constrained programming methodology to minimize total cost while minimizing environmental impact and maximizing social welfare. With the uncertain demand for bioenergy and the disruption in biorefinery, Salehi et al. (2022) presented a robust possibility programming model for designing biomass supply chain networks for maximizing profitability and customer satisfaction. To minimize unfulfilled demand, potential environmental risks, and emergency expenses on the upper level while maximizing survivor satisfaction on the lower level, Cao et al. (2021) presented a fuzzy tri-objective bi-level programming model.

Robust optimization methodology has been applied in biomass supply chain studies, where the uncertain parameter is distribution-free, and captured by an uncertainty set containing probable realization values of the uncertain parameter. Delkhosh and Sadjadi (2020) introduced a bi-objective robust optimization model considering economic and environmental aspects. Compared with the deterministic optimization model, it is demonstrated that the robust optimization model outperforms the deterministic model under all circumstances. Gumte et al. (2021a) introduced a data-driven robust optimization model to perform technological, environmental, and economic analyses for the biomass supply chains. In the proposed model, the uncertainty in bioenergy demand, price, and bio-waste supply is addressed using a data-driven robust optimization strategy. To handel the parameter uncertainty, Razm et al. (2021) proposed a robust optimization model for bioenergy supply chain planning. Computational results show that the robust solution is immune to inaccurate input data, which remains optimal, even if the parameters change slightly. Accounting for multiple uncertainties in the syngas supply chain based on forest biomass, Ahmadvand and Sowlati (2022) proposed a robust optimization model to obtain optimal decisions at the tactical level.

To clarify the differences between this study and the above literature, the related literature is classified in Table 1.

2.4. Research gap

Table 1 categorizes the related literature according to criteria of biomass type, product, sustainability, uncertain parameters, uncertainty modeling approach, and multi-objective solution method to determine the research gaps of current studies on the design of biomass supply chain networks. As shown in Table 1, previous literature has examined this issue using a deterministic optimization method; however, most studies are conducted in uncertain settings owing to the pervasiveness of uncertainty. Furthermore, in these uncertain studies, only the economic objective or both economic and environmental dimensions are considered. There are also a few relevant studies that consider environmental, social, and economic dimensions simultaneously. However, to the best of the authors' knowledge, there has been no research to date that takes the priority structure of environmental, social, and economic objectives into account in sustainable biomass supply chain planning and designed under the uncertainties associated with environmental and social impacts.

Specifically, the differences between the proposed optimization method in this paper and the existing literature are summarized as follows:

Table 1
Literature comparison related to this paper.

Literature	Biomass type	Product	Sustainability			Uncertain parameters			Uncertainty modeling approach	Multi-objective solution method
			Economic	Environmental	Social	Unit emission	Social score	Others		
Tesfamichael et al. (2021)	biomass	Biofuel	*						DP	
Wu et al. (2022)	Agri-biomas	Bioenergy	*						DP	
Kwon et al. (2022)	Organic waste	Biodiesel	*						DP	
Hombach et al. (2016)	Second-generation	Biodiesel	*	*					DP	
Mirhashemi et al. (2018)	Moringa oleifera	Biodiesel	*	*					DP	
Nandimandalam et al. (2022)	Renewable biomass	Electricity	*	*					DP	Augmented ϵ-constraint
Fernández-Puratich et al. (2021)	Agro-industrial wastes	Heat,power	*	*					DP	ϵ-constraint
Singh et al. (2022)	Waste animal fat	Biodiesel	*	*	*				DP	Augmented ϵ-constraint
Miret et al. (2016)	Corn,wood	Bioethanol	*	*	*				DP	Goal programming
Habib et al. (2020)	Waste animal fat	Biodiesel	*	*	*			*	RPP	ϵ-constraint
Gilani et al. (2020)	Sugarcane	Bioethanol	*	*	*			*	RPP	Fuzzy multi-objective method
Salehi et al. (2022)	Waste	Electricity	*	*	*			*	RPP	
Díaz-Trujillo et al. (2020)	Cow manure, Organicwastes, Wastewater	Biogas	*	*				*	SP	
Karimi et al. (2021)	Solid biomass	Power	*	*				*	SP	ϵ-constraint
Aranguren et al. (2021)	Agricultural biomass	Power	*					*	SP	
Guo et al. (2022)	Biomass	Bioenergy	*					*	SP	
Lo et al. (2021)	Biomass	Biogas	*	*				*	MC	
Simon et al. (2021)	Wood	Bioenergy	*					*	SM	
Ahmadvand and Sowlati (2022)	Forest-based biomass	Syngas	*					*	RO	
Razm et al. (2021)	Forest residues, agricultural waste	Bioenergy	*					*	RO	
Gumte et al. (2021a)	Bio-waste	Bioenergy	*	*				*	RO	ϵ-constraint
This paper	Agricultural straws, forest residues, livestock manures	Power	*	*	*	*	*		GRO	Goal programming

DP: deterministic programming, RPP: robust possibilistic programming, SP: stochastic programming, RO: robust optimization, GRO: globalized robust optimization, SM: simulation method, MC: Monte Carlo.

- Sustainability: In addition to standard carbon emissions, environmental variables including noxious gases and heavy metals are considered. Social variables including annual turnover, worker harm, and social acceptance are considered in addition to the typical job creation. In view of the worldwide concern for sustainable development, environmental, social, and economic objectives are separately considered as the first, second, and third priority levels, embodied in the proposed goal programming method.
- Uncertainty: Owing to the effects of the changeable environment and the cognitive level of decision-makers, both unit emissions and social scores are uncertain, which are characterized as a pair of uncertainty sets, respectively. Subsequently, the globalized robust optimization method is developed to model uncertain parameters because it is not only resistant to parameter uncertainty but also less conservative.

3. Problem statement

In this study, the SBPSC network, which is designed from the point of view of a green energy development company, consists of biomass supply sites, storage facilities, power generation plants, and demand zones, as shown in Fig. 2. To capture the effects of seasonality on biomass supply capacity, this study considers the SBPSC network design problem in a one-year planning horizon with twelve periods, i.e., one period per month. Different types of biomass, containing agricultural straws, forest residues, and livestock manures, are transported from supply sites to storage facilities and then to biomass power generation plants or directly to them. Storage facilities will incur some additional construction costs and storage costs to maintain inventories, but ensure a stable supply of biomass feedstock for these power generation plants during a planning horizon. At each power generation plant, a specific technology with a certain level of capability, such as LFGRS, Incinerator, AD, and ATT, needs to be built for a certain type of biomass, but at most one capability level of power generation technology for a given biomass can be selected.

Several decisions to be made in the SBPSC network include the following groups: locations of power plants and storage facilities, selections of power generation technologies in located power plants, biomass inventory level in each period, transportation quantities among biomass supply chain members in each period, as well as the quantities of biomass processed, electricity generated, and electricity allocated to demand zones in each period. Additionally, to achieve the sustainability of a biomass-based power generation supply chain network, three conflicting objectives of economy, environment, and society are considered simultaneously. Furthermore, the goal programming approach with a priority structure is employed to balance three conflicting objectives in this paper.

Table 2 provides notations and descriptions of the SBPSC network design problem, in which the considered uncertain parameters include unit emission and social score, and they are identified and selected by checking the impact of the uncertainty of multiple influencing parameters on the determinate model outputs using a local sensitivity analysis (LSA) approach (Ahmadvand and Sowlati, 2022). Refer to Appendix C for details. In what follows, several assumptions are described to formulate the SBPSC network design problem.

(A.1) All the electricity generated is acquired by a specialized power company at a predetermined price and then distributed to the areas in need. Therefore, the costs associated with power distribution are not considered.

(A.2) The processing of various types of biomass cannot be done using a single established technology, while it may be possible for a single type of biomass.

(A.3) If there is an overflow of biomass supply in the SBPSC network, then the excess biomass can be sold to other markets.

4. Globalized robust goal programming SBPSC model

To handle the uncertainty of unit emission and social score and consider economic, environmental, and social impacts, a globalized robust goal programming SBPSC model is formulated in this section.

4.1. General constraints

4.1.1. Capacity constraints

Constraint (1) assures that at most one power generation technology be built for processing a type of biomass at location j.

$$\sum_{k\in[K]}\sum_{r\in[R]} X_{jkmr} \le 1, \qquad \forall j \in [J], m \in [M]. \tag{1}$$

In each period, the biomass supply must not be greater than the supply capacity, which is represented by constraint (2).

$$\sum_{i\in[I]} F_{simt} + \sum_{j\in[J]} F_{sjmt} \le \eta_{mst}, \qquad \forall s \in [S], m \in [M], t \in [T]. \tag{2}$$

Constraints (3) and (4) show that the amounts of biomass holding and handling should not exceed the holding and handling capacities of the opened storage facilities, respectively.

$$\sum_{m\in[M]} e_m H_{imt} \le caph_i Y_i, \qquad \forall i \in [I], t \in [T]. \tag{3}$$

$$\sum_{m\in[M]}\sum_{j\in[J]} F_{ijmt} \le capf_i Y_i, \qquad \forall i \in [I], t \in [T]. \tag{4}$$

Constraint (5) reveals the power generation capacity of all technologies is limited.

$$V_{jkmt} \le \sum_{r\in[R]} capt_{kr} X_{jkmr}, \qquad \forall j \in [J], k \in [K], m \in [M], t \in [T]. \tag{5}$$

Constraint (6) indicates that the sum of electricity supplied by power generation plant j to all demand zones is less than the total amount of electricity generated.

$$\sum_{n\in[N]} Z_{jnt} \le Q_{jt}, \qquad \forall j \in [J], t \in [T]. \tag{6}$$

Constraint (7) ensures that the sum of electricity provided by all power plants to demand zone n is more than the demand.

$$\sum_{j\in[J]} Z_{jnt} \ge \xi_{nt}, \qquad \forall n \in [N], t \in [T]. \tag{7}$$

4.1.2. Constraints of flow balance

According to constraint (8), the biomass transported to power plant j must meet the amount used. Constraint (9) calculates the electricity generation of power plant j.

$$(1-\epsilon_m)\Big(\sum_{s\in[S]} F_{sjmt} + \sum_{i\in[I]} F_{ijmt}\Big) = \sum_{k\in[K]} V_{jkmt}, \quad \forall j \in [J], m \in [M], t \in [T]. \tag{8}$$

$$Q_{jt} = \sum_{k\in[K]}\sum_{m\in[M]} \lambda_{km} V_{jkmt}, \qquad \forall j \in [J], t \in [T]. \tag{9}$$

4.1.3. Inventory constraints

Constraints (10) and (11) ensure that the inventory level of biomass in period t is the sum of the remaining inventory after a deterioration in the preceding period and the input flow of biomass.

$$H_{imt} = \sum_{s\in[S]} F_{simt} - \sum_{j\in[J]} F_{ijmt}, \qquad \forall m \in [M], i \in [I], t = 1. \tag{10}$$

$$H_{imt} = (1-\gamma_m) H_{im(t-1)} + \sum_{s\in[S]} F_{simt} - \sum_{j\in[J]} F_{ijmt}, \quad \forall m \in [M], i \in [I], t \in [T]\backslash\{1\}. \tag{11}$$

4.1.4. Decision variable constraints

Eq. (12) is the binary constraint, and (13) is the nonnegative constraint.

$$X_{jkmr}, Y_i \in \{0,1\}, \qquad \forall i \in [I], j \in [J], k \in [K], r \in [R], m \in [M], \tag{12}$$

$$F_{simt}, F_{sjmt}, F_{ijmt}, H_{imt}, V_{jkmt}, Q_{jt}, Z_{jnt} \ge 0, \forall s \in [S], i \in [I], m \in [M], j \in [J], k \in [K], n \in [N], t \in [T]. \tag{13}$$

4.2. Globalized robust environmental goal constraint

The environmental impact of the SBPSC network is mainly assessed in terms of emissions and air pollution from biomass transportation and power production, including CO_2, VOC emissions, NO_x, and heavy metals. Since the unit costs of eliminating various pollutants are distinct, the total cost, rather than the total amount, is used to measure environmental impact, as shown in (14).

$$\Pi_1(\boldsymbol{\mu}, \boldsymbol{V}) = Emi_{tra} + \sum_{c\in[C]}\sum_{k\in[K]}\sum_{t\in[T]}\sum_{m\in[M]}\sum_{j\in[J]} \alpha_c \mu_{ck} V_{jkmt} = Emi_{tra} + \boldsymbol{\mu}^T \boldsymbol{V}, \tag{14}$$

Table 2
Notations and descriptions.

Notations	Descriptions
Index sets:	
$[S]$	Set of biomass supply sites, $s \in [S] = \{1, \dots, S\}$,
$[I]$	Set of potential storage facilities, $i \in [I] = \{1, \dots, I\}$,
$[J]$	Set of potential biomass power generation plants, $j \in [J] = \{1, \dots, J\}$,
$[M]$	Set of biomass types, $m \in [M] = \{1, \dots, M\}$,
$[N]$	Set of demand zones, $n \in [N] = \{1, \dots, N\}$,
$[K]$	Set of candidate power generation technologies, $k \in [K] = \{1, \dots, K\}$,
$[R]$	Set of capacity options of power generation technologies, $r \in [R] = \{1, \dots, R\}$,
$[T]$	Set of periods, $t \in [T] = \{1, \dots, T\}$,
$[G]$	Set of social factors, $g \in [G] = \{1, \dots, G\}$,
$[C]$	Set of emission types, $c \in [C] = \{1, \dots, C\}$,
$[L]$	Set of perturbation terms, $l \in [L] = \{1, \dots, L\}$.
Parameters:	
β_i	Fixed annual cost of opening a storage facility at site i (\$),
ψ_{jkr}	Fixed annual cost of establishing technology k with capacity level r at site j (\$),
ub_m	Unit purchasing cost of biomass m (\$/ton),
up_k	Unit operating cost using technology k (\$/ton),
uh_m	Unit holding cost of biomass m in a period (\$/ton),
dis_{si}	The distance between supply site s and storage facility i (km),
dis_{sj}	The distance between supply site s and biomass power plant j (km),
dis_{ij}	The distance between storage facility i and biomass power plant j (km),
$disuc$	Unit transportation cost (\$/km/ton),
η_{mst}	The amount of biomass m provided by supply site s in period t (ton),
$caph_i$	Capacity of storage facility i to hold biomass at each period (ton),
$capf_i$	Capacity of storage facility i in forwarding biomass to power plants in a period (ton),
$capt_{kr}$	Capacity of processing biomass by the technology k with level r in a period (ton),
ue	Unit price of electricity generated from biomass (\$/kWh),
e_m	Capacity utilization coefficient, i.e., the space needed for unit biomass m in storage facilities,
ϵ_m	Moisture content associated with biomass m,
λ_{km}	Conversion rate of power generation technology k from biomass m (kWh/ton),
γ_m	Deterioration rate of biomass m in storage facilities at each period,
κ_c	Unit emission of type c during transport process (kg/ton/km),
α_c	Unit cost of eliminating c (\$/kg),
w_g	The weight of social indicator g,
ξ_{nt}	The electricity needed by demand zone n in period t (kWh).
Uncertain parameters:	
ρ_{gkr}	The score on social indicator g of established technology k with capacity level r,
μ_{ck}	Unit emission of type c from processing biomass by technology k (kg/ton).
Decision variables:	
X_{jkmr}	Binary variable, if technology k with level r for processing biomass m is established at site j, it is 1; otherwise 0,
Y_i	Binary variable, if the storage facility is located at site i, it is 1; otherwise 0,
F_{simt}	Quantity of biomass m from supply site s to storage facility i in period t,
F_{sjmt}	Quantity of biomass m from supply site s to power plant j in period t,
F_{ijmt}	Quantity of biomass m from storage facility i to power plant j in period t,
H_{imt}	Quantity of biomass m holding at storage facility i in period t,
V_{jkmt}	Quantity of biomass m processing at power plant j using technology k in period t,
Q_{jt}	Quantity of electricity generated from power plant j in period t,
Z_{jnt}	Quantity of electricity provided by power plant j to demand zone n in period t.

where $Emi_{tra} = \sum_{c\in[C]} \alpha_c \kappa_c \big(\sum_{t\in[T]} \sum_{m\in[M]} \sum_{s\in[S]} \sum_{i\in[I]} dis_{si} F_{simt} + \sum_{t\in[T]} \sum_{m\in[M]} \sum_{s\in[S]} \sum_{j\in[J]} dis_{sj} F_{sjmt} + \sum_{t\in[T]} \sum_{m\in[M]} \sum_{i\in[I]} \sum_{j\in[J]} dis_{ij} F_{ijmt} \big)$ that denotes emissions during transportation, $\boldsymbol{\mu} = (\mu_{ck})_{c\in[C],k\in[K]}$, and $\boldsymbol{V} = (\alpha_c \sum_{t\in[T]} \sum_{m\in[M]} \sum_{j\in[J]} V_{jkmt})_{c\in[C],k\in[K]}$.

Decision-makers often expect the total cost of eliminating various pollutants to be as low as possible. Following the idea of the goal programming method, given an aspired goal g_1, the total cost Π_1 is expected not to exceed g_1 as far as possible. If Π_1 is greater than g_1, the segment exceeding g_1 should be minimized. Hence, decision-makers focus on the part in excess of g_1 and introduce the positive deviation d_1^+. Consequently, the environment objective (14) is formulated as a goal constraint (15),

$$\Pi_1(\boldsymbol{\mu}, \boldsymbol{V}) - d_1^+ \leq g_1. \tag{15}$$

In reality, a number of relevant factors, such as the quality of biomass, the energy production environment and the operational level of workers, contribute to the uncertainty of unit emissions. Acquiring accurate values of uncertain unit emissions is usually difficult, and the problem may worsen if little historical data is available. Therefore, the unit emission vector $\boldsymbol{\mu}$ is modeled under uncertainty and formulated as an affine function of perturbation vector $\boldsymbol{\zeta}^\mu$, that is, $\boldsymbol{\mu}(\boldsymbol{\zeta}^\mu) = \boldsymbol{\mu}^0 + \sum_{l\in[L]} \boldsymbol{\mu}^l \zeta_l^\mu$, where $\boldsymbol{\mu}^0$ is the nominal vector, $\boldsymbol{\mu}^l$ is a basic shift vector, $\boldsymbol{\zeta}^\mu$ is the perturbation vector. This formulation means that the uncertainty of $\boldsymbol{\mu}$ is caused by $\boldsymbol{\zeta}^\mu$, the dimension L of which is determined by the number of influence factors.

However, the crucial issue that how to characterize $\boldsymbol{\mu}$ has not been clear and should be addressed. The GRO method is a common tool to handle optimization problems which are influenced by parameter uncertainty. In the GRO method, the parameter uncertainty is characterized by an inter-outer uncertainty set. The key idea of the GRO method is that the feasibility must be met for the uncertain parameter values that belong to the inner uncertainty set analogous to the robust optimization, while the feasibility requirements are permitted to be violated but in a controlled way for the parameter values that are unlikely to occur.

Based on the above discussion, we consider two convex uncertainty sets $\mathcal{U}'_\mu$ and $\mathcal{U}_\mu$ with $\mathcal{U}'_\mu \subset \mathcal{U}_\mu$. For the realization of uncertain vector $\boldsymbol{\mu} \in \mathcal{U}_\mu \backslash \mathcal{U}'_\mu$, the constraint violation is allowed, but for the realization in $\mathcal{U}'_\mu$, the constraint must be satisfied. Therefore, the globalized robust environmental goal constraint is formulated as follows:

$$\Pi_1(\boldsymbol{\mu}, \boldsymbol{V}) - d_1^+ \leq g_1 + \min_{\boldsymbol{\mu}' \in \mathcal{U}_\mu'} \phi(\boldsymbol{\mu}, \boldsymbol{\mu}'), \qquad \forall \boldsymbol{\mu} \in \mathcal{U}_\mu, \tag{16}$$

where $\phi(\boldsymbol{\mu}, \boldsymbol{\mu}')$ is the distance between $\boldsymbol{\mu}$ and $\boldsymbol{\mu}'$. If $\boldsymbol{\mu} \in \mathcal{U}_\mu'$, then obviously $\phi(\boldsymbol{\mu}, \boldsymbol{\mu}') = 0$. For $\boldsymbol{\mu} \in \mathcal{U}_\mu \backslash \mathcal{U}_\mu'$, then $\phi(\boldsymbol{\mu}, \boldsymbol{\mu}') > 0$, which means violation of inequality (15) is allowed.

Remark 1. Constraint (16) is the globalized robust counterpart of the original uncertain constraint (15). While in the robust optimization method, it is required that uncertain constraint (15) holds for all vectors $\boldsymbol{\mu}$ in the outer uncertainty set $\mathcal{U}_\mu$, i.e.,

$$\Pi_1(\boldsymbol{\mu}, \boldsymbol{V}) - d_1^+ \leq g_1, \qquad \forall \boldsymbol{\mu} \in \mathcal{U}_\mu, \tag{17}$$

which is called robust environmental goal constraint. From a theoretical point of view, a solution that satisfies constraint (16) does not necessarily satisfy the constraint (17), which means that the feasible region of (16) includes that of (17). Therefore, the globalized robust optimization method can obtain a less conservative solution compared to the robust optimization method.

4.3. Globalized robust social goal constraint

To identify the social impact assessment, the S-LCA approach (Andrews, 2009) is commonly employed. Refer to the study of Fattahi et al. (2021), the social impacts of biomass-based power generation technologies are assessed using four indicators: job creation, social acceptance, annual turnover, and worker harm. Based on the above analysis, the social objective that reflects the social responsibility of the SBPSC network is as follows:

$$\Pi_2(\boldsymbol{\rho}, \boldsymbol{X}) = \sum_{g\in[G]} \sum_{k\in[K]} \sum_{r\in[R]} \sum_{j\in[J]} \sum_{m\in[M]} w_g \rho_{gkr} X_{jkmr} = \boldsymbol{\rho}^T \boldsymbol{X}, \tag{18}$$

where vector $\boldsymbol{\rho} = (\rho_{kr})_{k\in[K],r\in[R]}$ is uncertain (denote $\rho_{kr} = \sum_{g\in[G]} w_g \rho_{gkr}$ for convenience), and $\boldsymbol{X} = (\sum_{j\in[J]} \sum_{m\in[M]} X_{jkmr})_{k\in[K],r\in[R]}$.

Owing to the cognitive level of decision-makers, measurement error, and other factors, social indicator scores are difficult to determine exactly. On the principle of the goal programming method, the social objective is modeled as a globalized robust social goal constraint (19),

$$\Pi_2(\boldsymbol{\rho}, \boldsymbol{X}) + d_2^- \geq g_2 - \min_{\boldsymbol{\rho}' \in \mathcal{U}_\rho'} \phi(\boldsymbol{\rho}, \boldsymbol{\rho}'), \qquad \forall \boldsymbol{\rho} \in \mathcal{U}_\rho. \tag{19}$$

where g_2 is the aspired goal value of social objective that means the total social score should not be less than g_2 as much as possible, and d_2^- denotes the segment of social scores that is smaller than g_2. In addition, the convex uncertainty sets $\mathcal{U}_\rho' \subset \mathcal{U}_\rho$. For the realization of $\boldsymbol{\rho}$ in $\mathcal{U}_\rho'$, constraint (19) must be satisfied. In contrast, the constraint violation is all right for the values in $\mathcal{U}_\rho \backslash \mathcal{U}_\rho'$ but is controlled by the distance $\phi(\boldsymbol{\rho}, \boldsymbol{\rho}')$.

Remark 2. Using the robust optimization method, the social objective is modeled as a robust social goal constraint as follows:

$$\Pi_2(\boldsymbol{\rho}, \boldsymbol{X}) + d_2^- \geq g_2, \qquad \forall \boldsymbol{\rho} \in \mathcal{U}_\rho. \tag{20}$$

From constraints (19) and (20), the globalized robust optimization method allows controlled constraint violations in the outer uncertainty set while the robust optimization method requires the inequality holds for all realizations in the outer uncertainty set, so the globalized robust optimization method should be less conservative than the robust optimization method.

4.4. Economic goal constraint

The economic objective of the SBPSC network is to maximize profit, which is calculated as electricity sales revenue minus several general costs, as shown in (21).

$$\begin{aligned}
\Pi_3 = & \sum_{j\in[J]} \sum_{t\in[T]} Q_{jt} ue - \sum_{k\in[K]} \sum_{j\in[J]} \sum_{m\in[M]} \sum_{r\in[R]} \psi_{jkr} X_{jkmr} - \sum_{i\in[I]} \beta_i Y_i \\
& - \sum_{t\in[T]} \sum_{m\in[M]} \sum_{j\in[J]} \sum_{k\in[K]} up_k V_{jkmt} \\
& - \sum_{t\in[T]} disuc \left(\sum_{i\in[I]} \sum_{s\in[S]} \sum_{m\in[M]} dis_{si} F_{simt} + \sum_{j\in[J]} \sum_{s\in[S]} \sum_{m\in[M]} dis_{sj} F_{sjmt} \right. \\
& \left. + \sum_{i\in[I]} \sum_{j\in[J]} \sum_{m\in[M]} dis_{ij} F_{ijmt} \right) \\
& - \sum_{i\in[I]} \sum_{t\in[T]} \sum_{m\in[T]} uh_m H_{imt} - \sum_{t\in[T]} \left(\sum_{i\in[I]} \sum_{s\in[S]} \sum_{m\in[M]} ub_m F_{simt} \right. \\
& \left. + \sum_{j\in[J]} \sum_{s\in[S]} \sum_{m\in[M]} ub_m F_{sjmt} \right).
\end{aligned} \tag{21}$$

The first part in Eq. (21) expresses the sale revenue of power generated in the SBPSC network. The fixed costs of building power generation technologies are the second part. The third part is the fixed costs of building storage facilities. The operational costs for handling biomass at all power plants throughout the planning period make up the fourth part. The transportation cost is the fifth part. The inventory cost is the sixth term. The biomass purchase cost during the planning phase is the final term.

Based on the idea of goal programming, assuming the aspired goal value of the economic objective is g_3, then economic goal constraint is modeled as follows:

$$\Pi_3 + d_3^- - d_3^+ = g_3, \tag{22}$$

where d_3^- is the negative deviation which denotes the segment of profit lower than g_3, and d_3^+ is the positive deviation representing the segment of profit higher than g_3. Note that economic objective Π_3 is expected to be as big as possible, then d_3^- should be minimized.

Additionally, deviation variables meet the nonnegativity requirement,

$$d_1^+ \geq 0, d_2^- \geq 0, d_3^+ \geq 0, d_3^- \geq 0. \tag{23}$$

4.5. Globalized robust goal programming SBPSC model

In the context of sustainability, conflicting economic, environmental, and social goals have varying degrees of importance in the minds of decision-makers and are generally not achievable at the same time. In this situation, the modeling approach should incorporate a priority structure in three conflicting objectives depending on the current state policy and preference of decision-makers, thereby considering the goal programming method (Charnes and Cooper, 1961).

Given the growing worldwide environmental concerns, the top priority among the three conflicting objectives may be the environmental objective. Due to the requirements for sustainability, the social impact may be considered a higher priority than the economic objective. In other words, in the context of sustainable development, decision-makers first ensure that the environmental impact does not exceed the given aspired goal, then social responsibility, and finally try their best to achieve the economic goal value.

Therefore, in the SBPSC problem, the order of priority is environmental impact, social responsibility, and economic profit. Based on the above discussion, a globalized robust goal programming model (24) is developed for the SBPSC problem considering environmental, social, and economic objectives simultaneously, the objective function of which is to minimize the sum of deviations with priority levels,

$$\begin{aligned}
\min \quad & \mathbb{P}_1 d_1^+ + \mathbb{P}_2 d_2^- + \mathbb{P}_3 d_3^- \\
s.t. \quad & \text{Constraints } (1)\text{–}(13), (16), (19), (22), (23).
\end{aligned} \tag{24}$$

where $\mathbb{P}_1$, $\mathbb{P}_2$, and $\mathbb{P}_3$ are priority levels indicating the relative importance of environmental, social, and economic objectives, and the magnitude between them is $\mathbb{P}_1 \gg \mathbb{P}_2 \gg \mathbb{P}_3$.

Note that Eqs. (16) and (19) are all semi-infinite constraints caused by uncertain parameters. Examining model (24) and finding that solving the model directly would be difficult due to semi-infinite constraints. In Section 5, to overcome this difficulty, model (24) will be converted into an equivalent form through the Lagrange duality method, which can be solved directly by off-the-shelf software.

5. Tractable globalized robust counterpart SBPSC model

In this section, GRO methodology is employed to transform semi-infinite constraints (16) and (19) into a finite system of constraints, respectively, without shrinking the feasible region of the model (24).

5.1. Counterpart formulation of environmental goal constraint

As for the unit emission vector $\boldsymbol{\mu}$ in (16), its inner–outer uncertainty set $(\mathcal{U}'_\mu, \mathcal{U}_\mu)$ is given as follows:

$$\mathcal{U}'_\mu(\mathcal{U}_\mu) = \{\boldsymbol{\mu} = \boldsymbol{\mu}^0 + \sum_{l\in[L]} \boldsymbol{\mu}^l \zeta_l | \zeta \in \mathcal{Z}'_\mu(\mathcal{Z}_\mu)\}, \tag{25}$$

The outer uncertainty set $\mathcal{U}_\mu$ contains all possible values of $\boldsymbol{\mu}$, where nominal vector $\boldsymbol{\mu}^0$ is the center of the set. Shift matrix $\boldsymbol{A} = [\boldsymbol{\mu}^1 \cdots \boldsymbol{\mu}^L]$ is constituted of basic shifts. Perturbation vector ζ varies in the perturbation sets $\mathcal{Z}'_\mu = \{\zeta | \|\zeta\|_1 \le \Gamma_\mu, \|\zeta\|_\infty \le \tau'_\mu\}$, and $\mathcal{Z}_\mu = \{\zeta | \|\zeta\|_\infty \le \tau_\mu\}$ with $0 \le \tau'_\mu \le \tau_\mu$, which indicates that $\mathcal{Z}'_\mu \subset \mathcal{Z}_\mu$ implying $\mathcal{U}'_\mu \subset \mathcal{U}_\mu$. $\boldsymbol{\mu}$ is fixed at its nominal vector $\boldsymbol{\mu}^0$ when $\boldsymbol{\zeta} = \mathbf{0}$.

Due to limited data available, only nominal values and support information about uncertain unit emissions can be obtained. Then the outer uncertainty set (i.e., a box set) bound can be determined based on known nominal values and support information. However, the box is too pessimistic, so the inner uncertainty set (i.e., a budget set) is introduced to reduce the conservatism level of the solution. The inner–outer uncertainty set falls somewhere in between, which is not only less conservative but also more flexible in adjusting the robustness of the method against the level of conservatism of the solution. The bounds of the inner uncertainty set can be chosen and adjusted by decision-makers based on their conservatism attitudes or some other presumable information about uncertain parameters.

Theorem 1. *For uncertain unit emission vector $\boldsymbol{\mu}$, let the distance function $\phi(\boldsymbol{\mu}, \boldsymbol{\mu}') = \alpha(\|\boldsymbol{\mu} - \boldsymbol{\mu}'\|_\infty)$, with $\alpha(t) = \theta_\mu t$, where $t \ge 0, \theta_\mu \ge 0$. Based on uncertainty sets $\mathcal{U}'_\mu$ and $\mathcal{U}_\mu$, as indicated in (25), the computationally tractable formulation of constraint (16) can be expressed as the following finite system of constraints,*

$$\begin{cases} (\boldsymbol{\mu}^0)^T \boldsymbol{V} + \Gamma_\mu \|\boldsymbol{e}\|_\infty + \tau'_\mu \|\boldsymbol{f}\|_1 + \tau_\mu \|\boldsymbol{A}^T \boldsymbol{v}\|_1 \le d_1^+ + g_1 - Emi_{tra} & (a) \\ \boldsymbol{e} + \boldsymbol{f} = \boldsymbol{A}^T \boldsymbol{w} & (b) \\ \boldsymbol{v} + \boldsymbol{w} = \boldsymbol{V} & (c) \\ \|\boldsymbol{w}\|_1 \le \theta_\mu & (d) \end{cases} \tag{26}$$

where $\boldsymbol{e}$, $\boldsymbol{f}$, $\boldsymbol{w}$, and $\boldsymbol{v}$ are introduced variables, $Emi_{tra} = \sum_{c\in[C]} \alpha_c \kappa_c (\sum_{s\in[S]} \sum_{i\in[I]} \sum_{m\in[M]} \sum_{t\in[T]} dis_{si} F_{simt} + \sum_{s\in[S]} \sum_{j\in[J]} \sum_{m\in[M]} \sum_{t\in[T]} dis_{sj} F_{sjmt} + \sum_{i\in[I]} \sum_{j\in[J]} \sum_{m\in[M]} \sum_{t\in[T]} dis_{ij} F_{ijmt})$.

Proof. Refer to Appendix A for proof. □

Theorem 1 gives the tractable formulation for constraint (16), which means that replacing constraint (16) in the model (24) with the system (26) would contribute to the computational tractability of this model.

5.2. Counterpart formulation of social goal constraint

Regarding uncertain social score vector $\boldsymbol{\rho}$, its inner–outer uncertainty set $(\mathcal{U}'_\rho, \mathcal{U}_\rho)$ depends on the perturbation set $(\mathcal{Z}'_\rho, \mathcal{Z}_\rho)$, as shown in Eq. (27),

$$\mathcal{U}'_\rho(\mathcal{U}_\rho) = \{\boldsymbol{\rho} = \boldsymbol{\rho}^0 + \sum_{l\in[L]} \boldsymbol{\rho}^l \zeta_l | \zeta \in \mathcal{Z}'_\rho(\mathcal{Z}_\rho)\}. \tag{27}$$

The nominal vector $\boldsymbol{\rho}^0$ is the center of the uncertainty set. The shift matrix is consisted of basic shifts, namely $\mathbf{B} = [\boldsymbol{\rho}^1 \cdots \boldsymbol{\rho}^L]$. Perturbation vector lies in the perturbation sets $\mathcal{Z}'_\rho = \{\zeta | \|\zeta\|_1 \le \Gamma_\rho, \|\zeta\|_\infty \le \tau'_\rho\}$, and $\mathcal{Z}_\rho = \{\zeta | \|\zeta\|_\infty \le \tau_\rho\}$ with $0 \le \tau'_\rho \le \tau_\rho$. Obviously, $\mathcal{Z}'_\rho \subset \mathcal{Z}_\rho$ implying $\mathcal{U}'_\rho \subset \mathcal{U}_\rho$. Particularly, when $\boldsymbol{\zeta} = \mathbf{0}$, $\boldsymbol{\rho}$ is fixed at its nominal vector $\boldsymbol{\rho}^0$. For the selection of perturbation sets, refer to Remark 3.

In general, the uncertain social score vector $\boldsymbol{\rho}$ depends on the subjective judgment of experts. According to the given nominal values and support information, the determinations of bounds of the inner and outer uncertainty sets can refer to the case of $\boldsymbol{\mu}$.

Theorem 2. *For uncertain social scores $\boldsymbol{\rho}$, let the distance function $\phi(\boldsymbol{\rho}, \boldsymbol{\rho}') = \alpha(\|\boldsymbol{\rho} - \boldsymbol{\rho}'\|_\infty)$ with $\alpha(t) = \theta_\rho t$, where $t \ge 0, \theta_\rho \ge 0$. Based on uncertainty sets $\mathcal{U}'_\rho$ and $\mathcal{U}_\rho$, as shown in (27), the computationally tractable formulation of constraint (19) is expressed as the following finite system of constraints,*

$$\begin{cases} (\boldsymbol{\rho}^0)^T \boldsymbol{X} - \Gamma_\rho \|\boldsymbol{c}\|_\infty - \tau'_\rho \|\boldsymbol{d}\|_1 - \tau_\rho \|\boldsymbol{B}^T \boldsymbol{\varphi}\|_1 \ge g_2 - d_2^- & (a) \\ \boldsymbol{c} + \boldsymbol{d} = \boldsymbol{B}^T \boldsymbol{\sigma} & (b) \\ \boldsymbol{\varphi} + \boldsymbol{\sigma} = \boldsymbol{X} & (c) \\ \|\boldsymbol{\sigma}\|_1 \le \theta_\rho & (d) \end{cases} \tag{28}$$

where $\boldsymbol{c}$, $\boldsymbol{d}$, $\boldsymbol{\varphi}$, and $\boldsymbol{\sigma}$ are introduced variables.

Proof. Refer to Appendix A for proof. □

Theorem 2 shows the finite system (28) is an equivalently tractable form of (19). Hence, the semi-infinite constraint (19) in the model (24) is replaced by the system (28), allowing off-the-shelf software to directly solve this model.

Remark 3. The reasons for choosing box & budget sets are as follows. (1) Due to limited data available, only nominal values and support information of uncertain parameters can be obtained. (2) The budget uncertainty set has computational advantages. (3) The budget uncertainty set implies a probability guarantee in the case that random perturbation variables are independent and symmetrically distributed in [−1,1]. However, if there are plenty of data available, data driven approaches (Gumte et al., 2021b; Inapakurthi et al., 2020; Pantula and Mitra, 2020; Sharma et al., 2021) have a greater advantage in accurately characterizing data uncertainty.

5.3. Tractable globalized robust counterpart SBPSC model

In light of Theorems 1 and 2, the tractable counterpart form of the proposed globalized robust goal programming SBPSC model (24) is as follows:

$$\begin{aligned} \min \quad & \mathbb{P}_1 d_1^+ + \mathbb{P}_2 d_2^- + \mathbb{P}_3 d_3^- \\ s.t. \quad & \text{Constraints (1)–(13),(22),(23),(26),(28).} \end{aligned} \tag{29}$$

In summary, after deriving the counterparts of semi-infinite constraints (16) and (19), the computationally intractable model (24) is equivalently reformulated as model (29), which is a MILP model and can be solved by off-the-shelf software directly.

6. Case study

To confirm the viability and efficacy of the proposed globalized robust goal programming method, a case study is conducted. In this section, the case description and data resources are presented.

6.1. Case description

According to the data from the Ministry of Land and Resources of China, the cultivated land area in Hubei Province was approximately 5,245.27 thousand hectares, and the actual operating woodland area was approximately 6260.55 thousand hectares by the end of 2016. As an agricultural and forestry province in China, Hubei Province is rich in biomass resources, such as agriculture straws, forest residues, and livestock manures. However, owing to the low utilization rate, large amounts of biomass energy are wasted in the fields and forests and directly buried as fertilizers.

Under the conditions of implementing the new strategy for national energy security and carbon reduction targets, the Chinese government and local authorities are always in effect to encourage and promote biomass-based power generation and provide some preferential policies. So far, a few biomass-based power plants have been established in Hubei Province. However, the overall production is low, and the scale of operations is small. The main hurdle faced by these power plants is the scarcity of biomass energy. For instance, Laifeng Kaidi Green Energy Development Co., LTD. engages in biomass power generation, in which power generation fuel is mainly straw, shrubs, and other fuels. The current daily consumption is 1000 tons; however, the purchase amount is only 300 tons, implying that it takes three days to collect enough fuel to generate electricity for one day.[1]

In view of the existing issues in the biomass-based power generation industry in Hubei Province, it is necessary to make an overall project plan. This paper aims to optimize the design of a sustainable biomass-based power supply chain network in Hubei Province by proposing plans for the location of biomass power plants and storage facilities, determining transportation amounts, inventory levels, and power generation. Meanwhile, this case study also verified that the proposed model and method are feasible and effective.

6.2. Data collection and estimation

This study considers three types of biomass feedstock, agriculture straws, forest residues, and livestock manures as the primary sources for power generation. The availabilities of agriculture straws, forest residues, and livestock manures are annually around 30 million tons, about 4 million tons, and approximately 1.8 million tons produced, respectively, based on data from the Hubei Provincial Department of Agriculture and Rural Affairs, Hubei Forestry Bureau, and Hubei Provincial Statistics Bureau. Note that livestock manures are available year around, while agricultural straws and forest residues can only become available throughout the year except the winter, and the majority of agricultural residues are primarily obtained in the summer and fall.

In total, 40 feedstock sites with prominent agriculture or forestry are considered as the biomass suppliers. The locations of 40 feedstock suppliers and the availability of three types of feedstock are shown in Fig. 3. Owing to the seasonality of biomass feedstock, there is a need to create storage facilities in the biomass supply chain to provide feedstock for power plants during the off-season. In this case, 12 potential storage facilities, which are also potential power plants, are considered, as shown in Fig. 4.

Without considering the location, the average annualized cost of opening a storage facility with a holding capacity of 0.8 million tons and a forwarding capacity of 1.5 million tons per period is roughly \$3.42 million (Fattahi et al., 2021). During storage in a period, the rates of deterioration for agricultural straws, forest residues, and livestock manures are 0.015, 0.03, and 0.04, and the capacity utilization factors are 1.15, 1.05, and 1.10, respectively. For further information regarding biomass, see Table B.1.

The large-sized truck is chosen as the transportation mode in accordance with the properties of biomass, and the unit transport cost is fixed at 0.075 (\$/km/ton). The distances between arbitrary two entities are acquired through Baidu map (api.map.baidu.com), which are listed in Tables B.2 and B.3. There are four different generation technologies available for each biomass-based power plant: LFGRS, Incinerator, AD, and ATT. For each technology, three levels of capacity are considered, namely large, medium, and small, and their capacities of processing biomass in a period are 8×10^5, 6×10^5, and 4×10^5 (ton), respectively. The unit operating costs of LFGRS, Incinerator, AD, and ATT are 5.2, 5.8, 4.3, and 6.0 (\$/ton), respectively (Fattahi et al., 2021). For more information on the technology, see Tables B.4 and B.5. According to National Development and Reform Commission records, the unit power price of agricultural and forestry biomass after subsidies is 0.1095 (\$/kWh).

According to the Hubei Province's 2021 Statistical Yearbook, the total amount of electricity consumed in 2020 was 218.4 billion kWh, with consumptions for agriculture, forestry, animal husbandry and fishery, wholesale and retail trade, industry, and residents amounting to approximately 4.2, 35.8, 134.5, and 43.9 billion kWh, respectively. In this case, about 5% of the electricity consumption of the four industries is taken as the annual demand, which is randomly allocated to 12 months, as shown in Table B.6.

This study mainly considers four types of emissions, which are NO_x, VOC emissions, CO_2, and heavy metals. Referring to Fattahi et al. (2021), the unit costs of eliminating NO_x, VOC emissions, CO_2, and heavy metals are 5.7, 4.4, 0.023, 9121 (\$/kg), respectively. The unit emissions of NO_x, VOC emissions, CO_2, and heavy metals during transport are in order 0.031, 0.0051 0.2002, 0 (kg/ton/km). In addition, the unit emissions in the power generation using different technologies are shown in Table B.7, which are regarded as nominal values. The basic shifts are assumed as 5% of the corresponding nominal values (Feng et al., 2022).

To quantify the social impact of various technologies, four social indicators, such as job creation, annual turnover, social acceptance, and worker harm, are chosen based on the S-LCA approach. Then, the fuzzy analytical hierarchy procedure is used to generate the score of power generation technology k with capacity level r concerning social indicator g (Fattahi et al., 2021). In more detail, the pairwise matrix is built for every social indicator based on the judgement of experts, after which experts choose the linguistic preferences for technologies, which are expressed as triangular fuzzy numbers, and finally the social score of technologies on each social indicator is calculated. Table B.5 displays the final outcomes, which are nominal values $(\sum_c w_c \rho_{ckr})^0$ of uncertain social scores. The basic shifts $(\sum_c w_c \rho_{ckr})^l$ are all assumed to be 5% of the nominal values.

7. Computational results and analysis

This section presents numerical results and managerial insights. All numerical experiments are solved by CPLEX 12.8.0 optimization software on a computer (Inter(R) Core(TM) i5-10210U, 1.60 GHz and 16 GB RAM) with Windows 10 operating system.

7.1. Computational results

Before computational experiments, assume that the priority levels of environmental, social, and economic objectives are as follows: $\mathbb{P}_1 = 10^8$, $\mathbb{P}_2 = 1$, $\mathbb{P}_3 = 10^{-8}$. For more reasonable results, by reference to optimal values of corresponding single-objective models, the aspired goal values of three objectives are set to $g_1 = 1.96{\times}10^9$, $g_2 = 350$, and $g_3 = 3.65{\times}10^8$, respectively. In practice, decision-makers can set aspired goal values of environmental and social objectives according to the quotas and requirements of the environmental protection department and human resources department, and set the aspired goal value of the economic objective based on the development of the enterprise itself. In order

[1] http://tjj.hubei.gov.cn/tjsj/

(a) Agricultural straws

(b) Forest residues

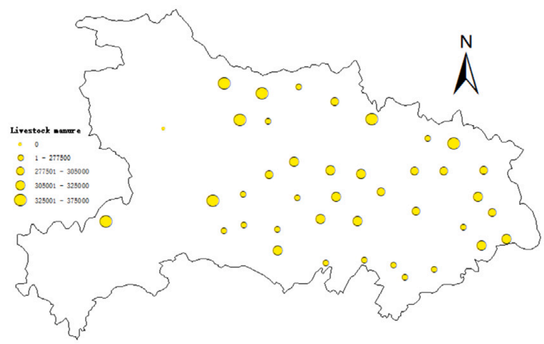

(c) Livestock manures

Fig. 3. The amount of biomass available at each supplier.

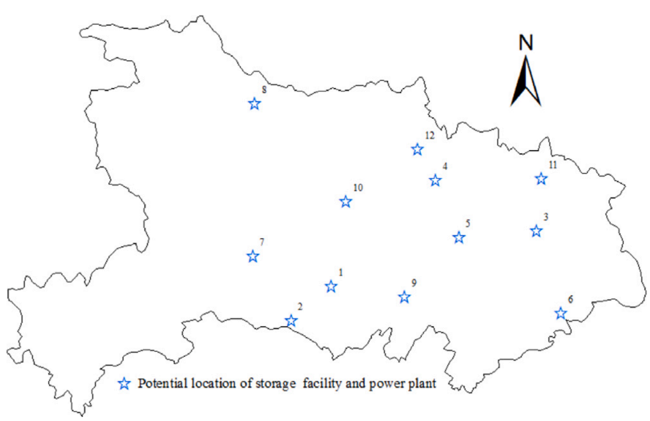

Fig. 4. Potential locations of the storage facility and biomass-based power generation plant.

to facilitate research, the parameters associated with two inner–outer uncertainty sets are assumed to be the same, that is, $\theta_\mu = \theta_\rho = \theta$, $\Gamma_\mu = \Gamma_\rho = \Gamma$, $\tau_\mu = \tau_\rho = \tau$, and $\tau'_\mu = \tau'_\rho = \tau'$. Besides, $\theta = 1, \tau = 1, \tau' = 0.7, \Gamma = 1.5$.

The optimal value for the proposed globalized robust goal programming SBPSC model is 0.642, with the deviation variables as follows:

$d_1^+ = 0, d_2^- = 0, d_3^- = 6.4157 \times 10^7$.

According to the calculation result, the environmental and social aspired goals have all been met, but the economic goal has not. Actually, the realization value of the environmental objective is 1.96×10^9, which does not exceed and equals its aspired goal, the social objective is 1134.8, which exceeds the given aspired goal, and the economic objective is 3.0084×10^8, which has not achieved its aspired goal. The reason may be that the economic objective is regarded as having the lowest priority among the three objectives. Next, the results of location strategies for storage facilities and biomass-based power plants and the selection of generation technologies in located power plants are reported in Table 3. In order to facilitate, agricultural straws, forest residues, and livestock manures are denoted as biomass 1, 2, and 3, respectively.

From Table 3, locations 1, 3, 4, 5, 6, 7, 8, 10, and 11 are selected as storage facilities, and locations 1, 3, 4, 6, 7, 8, 10, 11, and 12 are chosen to establish power plants. It is found that a storage facility is built at location 5, but no power plant is built; location 12 does not have a storage facility, but it is selected as a power plant. The reason may be that the power plants near location 5 need more biomass in the off-season of biomass harvesting, so location 5 is established to provide enough biomass for them. Yet the biomass needed for the power plant built at location 12 is provided by nearby suppliers and storage facilities, it is unnecessary to establish a storage facility here.

Besides, the fourth column of Table 3 presents the selection of generation technologies for each power plant built. It is noted that technology ATT is the most widely used choice in the power generation plants. There are only a few power plants that have chosen LFGRS and Incinerator. None of the power plants select technology AD, however. It might be because, while having the highest annualized fixed cost and unit operating cost, technology ATT produces the most electricity per unit of biomass. Despite having the lowest unit operating cost, AD's annual fixed cost is second only to ATT.

According to the computational results, under the given environmental and social aspired goals, the economic objective is 3.0084×10^8. The costs include strategic costs, i.e., the costs of building storage facilities and power generation technologies, as well as tactical costs, as shown in Fig. 5. From Fig. 5, the cost of procurement is the most, approximately 4.11×10^8, the transportation cost is next, about 2.23×10^8, the cost of operation related to power generation technologies is about 1.18×10^8, and the inventory cost is the least, approximately 2.32×10^7.

Table 3
Location strategies and selection of technologies.

Potential locations	Selected storage facilities	Selected power plants	Selected technology and its capacity
1	1	1	biomass 1: ATT (large), biomass 3: LFGRS (large)
2	~	~	~
3	3	3	biomass 1: ATT (large)
4	4	4	biomass 3: ATT (large)
5	5	~	~
6	6	6	biomass 2: ATT (medium), biomass 3: LFGRS (large)
7	7	7	biomass 1: Incinerator (large), biomass 3: ATT (large)
8	8	8	biomass 1: Incinerator (large), biomass 3: Incinerator (large)
9	~	~	~
10	10	10	biomass 3: ATT (small)
11	11	11	biomass 1: ATT (small), biomass 2: ATT (large), biomass 3: Incinerator (medium)
12	~	12	biomass 1: ATT (large), biomass 3: LFGRS (large)

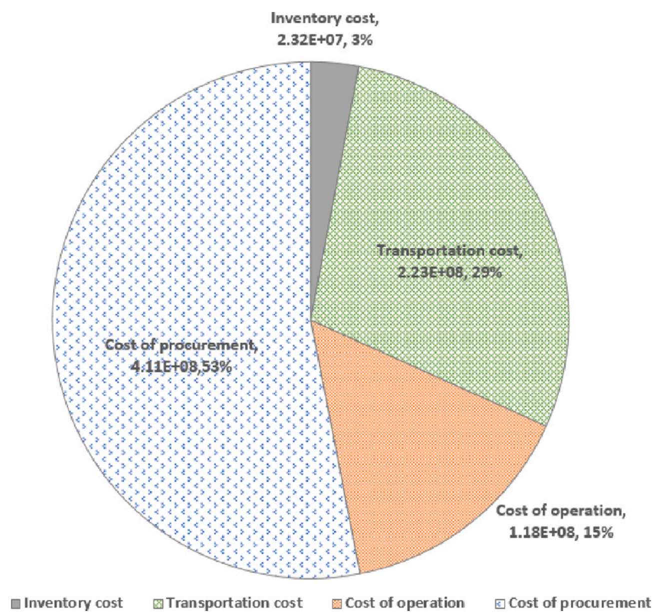

Fig. 5. Division of total tactical costs across the supply chain.

The cost of acquiring biomass makes up around 53% of the total tactical costs. Additionally, the costs associated with transportation, technology operation, and inventory are 29%, 15%, and 3%, respectively. It is found that the network design and logistics planning in the SBPSC problem are significant.

7.2. The comparisons of different optimization models

7.2.1. Comparative result and analysis

To illustrate the performance of the proposed globalized robust goal programming model (GRO model), two sets of comparison experiments with the robust goal programming model (RO model) and the nominal goal programming model (nominal model) are conducted. In the RO model, uncertain parameters $\boldsymbol{\mu}$ and $\boldsymbol{\rho}$ belong to the uncertainty sets $\mathcal{U}_\mu$, and $\mathcal{U}_\rho$, respectively, which are viewed as the outer uncertainty sets in the context of the GRO method. In the nominal model, $\boldsymbol{\mu}$ and $\boldsymbol{\rho}$ are all known and determinate, which are assumed to be their nominal values $\boldsymbol{\mu}^0$ and $\boldsymbol{\rho}^0$, respectively.

We solve GRO, RO, and nominal models under the same priority levels and aspired goal values as those in Section 7.1 to effectively compare their performances. Regarding the GRO model, we conduct three different sets of numerical experiments under different parameters, where the parameters in Case 1: $\theta = 1, \tau = 1, \tau' = 0.7, \Gamma = 1.5$; Case 2: $\theta = 2, \tau = 1, \tau' = 0.6, \Gamma = 0.85$; and Case 3: $\theta = 4, \tau = 1, \tau' = 0.7, \Gamma =$ 1.5. Optimal values and deviation variables of different optimization models are shown in Table 4.

Table 4
Deviation variables and optimal values of different optimization models.

Model	Case	d_1^+	d_2^-	d_3^-	Optimal value
Nominal model		0	0	0	0
RO model		0	0	1.5468×10^8	1.547
	Case 1	0	0	6.4157×10^7	0.642
GRO model	Case 2	0	0	4.9914×10^7	0.499
	Case 3	0	0	8.1707×10^7	0.817

Table 4 shows that environmental, social, and economic objectives all achieve the stated aspired goals by the computation of the nominal model. However, the current solution will no longer be optimal or even unfeasible when there is any fluctuation in the data caused by external factors. The solution of nominal model cannot hedge against the parameter uncertainty, whereas RO model and GRO model do. The calculation for the RO model shows that environmental and social objectives have both achieved the given aspired goals, but the economic objective has not. The deviation variable of the economic objective is 1.5468×10^8, which indicates that the part realized is only about 60% of the given aspired goal. Apparently, the solution of the RO model is uncertainty-immunized, but it is too conservative.

The findings of the GRO model show that environmental and social objectives always meet the stated aspired goals, and the deviation variables associated with the economic objective are 6.4157×10^7, 4.9914×10^7, and 8.1707×10^7 in the conditions of Cases 1, 2, and 3, respectively. Under these three cases, the realized economic profit of the GRO model is approximately 42.5% higher than that of the RO model on average. In general, the deviation variables obtained from the GRO model are always less than that from the RO model. In other words, the GRO model can achieve larger economic objectives compared with the RO model. Hence, not only can the GRO model resist data uncertainty, but also is less conservative than the RO model. Furthermore, the choice of parameters about the uncertainty set will influence the conservatism degree of the GRO solution. One such example is the globalized sensitivity parameter θ, which in Case 1 is set to 1 and in Case 3 is 4, resulting in a larger optimal value (i.e., 0.817) in Case 3.

Then we continue to present the comparison results about the location strategies of storage facilities and power generation plants obtained from nominal, RO, and GRO models, as shown in Fig. 6. From Fig. 6, the location strategies under various models are different. When the data are known accurately, the location strategy obtained by the nominal model is shown in Fig. 6(a), where eight storage facilities are opened at locations 3, 5, 6, 7, 8, 10, 11, and 12, respectively; seven power plants are established at locations 1, 2, 3, 4, 7, 8, and 10. However, from Fig. 6(b), the RO model seems to be more cautious in its siting decisions, with eleven storage facilities and eleven power plants, including almost all the candidates. The RO model could hedge

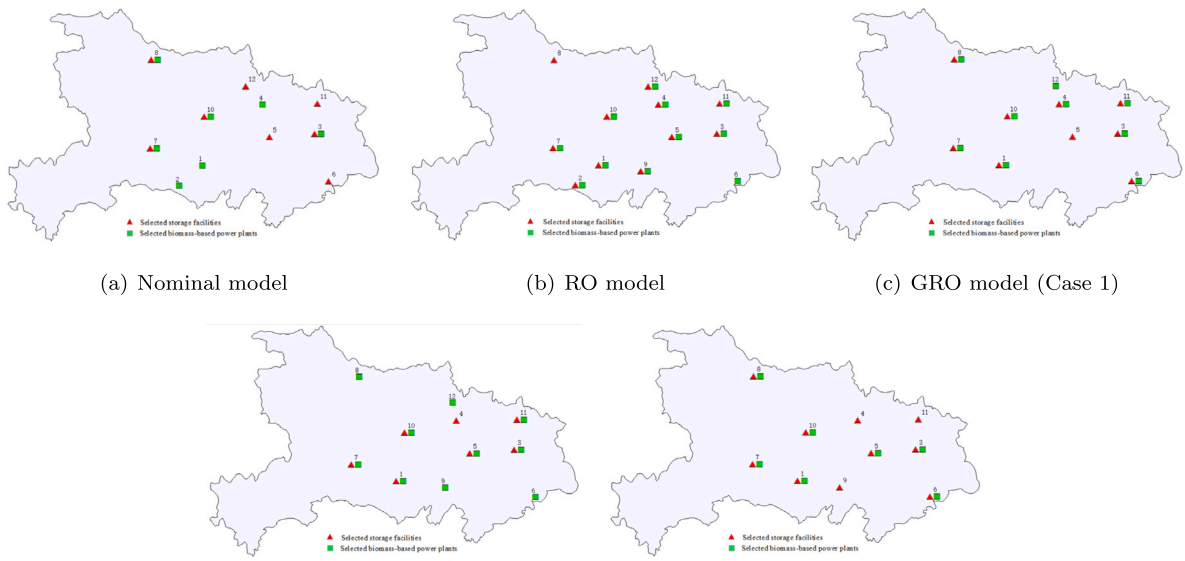

(a) Nominal model (b) RO model (c) GRO model (Case 1)

(d) GRO model (Case 2) (e) GRO model (Case 3)

Fig. 6. Location strategies under different optimization models.

against data uncertainty compared to the nominal model, but it is too conservative.

Moreover, from Fig. 6(c), (d), and (e), we find that the location strategies solved by the GRO model are always less conservative than that of the RO model in the situations of Cases 1, 2, and 3 just in terms of the located site numbers. Considering Case 1, which is shown in Fig. 6(c). There are nine storage facilities established, which are locations 1, 3, 4, 5, 6, 7, 8, 10, and 11, respectively; and nine power generation plants built are located at sites 1, 3, 4, 6, 7, 8, 10, 11, and 12. The details of this set of solutions are reported in Section 7.1.

Fig. 7 shows the monthly power generation obtained from different optimization models. The GRO model result is presented here in the situation of Case 1. The monthly power generation under various models, as shown in Fig. 7, largely mirrors the seasonality of the biomass supply, with more power generated during harvest season than during the off-season. Compared with other two models, the monthly power generation under the RO model is almost the least, which may be related to the greatest deviation variable of the economic objective under the RO model. Interestingly, while the deviation variable of economic objective under the GRO model is greater than that under the nominal model, the total power generation under the GRO model is greater than that under the nominal model.

In conclusion, the nominal model is the best choice when the parameters are known accurately. However, in the complex real world, affected by many factors, it is difficult to acquire uncertain parameters accurately. In this case, RO and GRO models are preferred by decision-makers due to their characteristics of uncertainty-immunized. In many cases, the RO approach is too conservative. Therefore, the GRO approach is a good choice when the parameters are uncertain, and decision-makers want to obtain a robust SBPSC network structure that can resist parameter uncertainty without being overly conservative.

7.2.2. Simulation validation and analysis

In this section, the realization-based simulation method is used to assess the effectiveness and desirability of the proposed GRO model, which can handle parameter uncertainty while being less conservative than the RO model.

Taking the uncertain social goal constraint as an example, this study uses the violation probability (VP) to measure the ability of different model solutions to hedge against the parameter uncertainty, which is as follows:

$$VP = \frac{1}{N}\sum_{n\in N}\mathbb{1}\Big(\sum_{k\in[K]}\sum_{r\in[R]}\sum_{j\in[J]}\sum_{m\in[M]}\rho_{kr}^{n}X_{jkmr} + d_2^- < g_2\Big),$$

where N is sample size, ρ_{kr}^n is the n th sample of uncertain parameter ρ_{kr}, $\mathbb{1}(\cdot)$ is 1 if the inequality is true, 0 otherwise. See Section 7.2.1 for solutions X_{jkmr} and d_2^- of different models.

Specifically, assuming that the social score ρ_{kr} uniformly changes by ±50% from its nominal value, then N simulated cases are sampled from the uniform distribution $[50\%\rho_{kr}^0, 150\%\rho_{kr}^0]$, where ρ_{kr}^0 is the nominal value of ρ_{kr}. In this experiment, sample sizes are set to 50, 100, and 200, respectively. For each case, 20 groups of sample values are uniformly sampled from the range $[50\%\rho_{kr}^0, 150\%\rho_{kr}^0]$, and the constraint violation probabilities of these 20 groups of samples under the three optimization models are programmed and calculated. Furthermore, the maximum, minimum, average, and standard deviation of these 20 violation probabilities under each optimization model can be acquired. Statistics of the violation probability under different optimization models are shown in Table 5.

From Table 5, several matters are observed as follows. (1) The violation probability of the nominal model is obviously higher than those of the GRO and RO models. For instance, when $N = 50$, the average violation probability of the nominal model is 0.5665, while the average violation probabilities of the GRO and RO models are 0.0363 and 0.0030, respectively. This means that the optimal solution of the nominal model is no longer feasible when uncertain parameters fluctuate in most instances. Compared to the nominal model, the lower violation probability indicates that the GRO and RO methods can resist parameter uncertainty. (2) However, the RO method appears to be too conservative because its violation probabilities are almost zeros. It is really the case that the realized economic goal of the RO model is only about 60% of the aspired goal value, as shown in Section 7.1. (3) The average violation probabilities of the GRO model are slightly higher than the RO model, which means the GRO method is less conservative. As described in Section 7.1, the GRO model achieves an economic goal that is 42.5% higher than the RO model on average, confirming the effectiveness and desirability of the proposed model. (4) Moreover, the standard deviation of the GRO model decreases with an increase in the sample size, which verifies the stability of the GRO method.

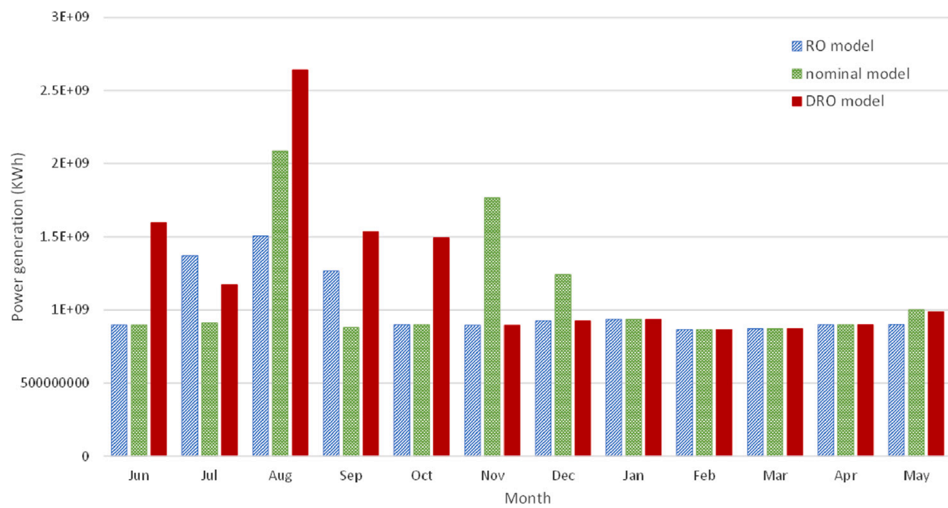

Fig. 7. Comparison of monthly power generation under different models.

Table 5
Statistics of the constraint violation probability under different optimization models.

Sample size N	Model	Statistical indicators (VP)			
		Max.	Min.	Avg.	StD.
50	nominal	0.6600	0.4600	0.5665	0.0485
	GRO	0.0800	0.0000	0.0363	0.0209
	RO	0.0200	0.0000	0.0030	0.0071
100	nominal	0.5800	0.4900	0.5520	0.0389
	GRO	0.0600	0.0100	0.0290	0.0164
	RO	0.0100	0.0000	0.0020	0.0040
200	nominal	0.6050	0.5100	0.5570	0.0312
	GRO	0.0500	0.0150	0.0300	0.0097
	RO	0.0100	0.0000	0.0015	0.0032

In conclusion, the simulation results demonstrate that the proposed globalized robust goal programming SBPSC model is a superior approach to handling uncertainty in the presence of data uncertainty without being overly conservative.

7.3. Effects of some parameters

This section investigates the effects of some significant parameters on the results of the proposed model. The environmental, social, and economic objectives still take the priority levels of $\mathbb{P}_1 = 10^8$, $\mathbb{P}_2 = 1$, $\mathbb{P}_3 = 10^{-8}$. The parameters associated with the uncertainty set are as follows: $\theta = 1, \tau = 1, \tau' = 1, \Gamma = 1.5$.

7.3.1. Effects of aspired goals

Assuming that fixed social and economic aspired goals are 350 and 3.65×10^8, respectively, the impacts of changing the environmental aspired goal on the optimal value and realization value of the economic goal are observed. Then, the environmental and economic aspired goals are 1.96×10^9 and 3.65×10^8, respectively, and the effects of social aspired goal on the optimal value and realization value of the economic goal are studied.

As shown in Fig. 8(a), when the environmental goal is increased from 1.860×10^9 to 1.869×10^9, there is a non-increasing monotonic trend in the optimal value, and the economic profit is not always achieved the aspired goal value. The corresponding optimal value reflects the portion which the economic aspired goal is not achieved. In other words, with the increase of the environmental aspired goal, the realization value of the economic goal is increasing. The reason may be that the larger environmental aspired goal means looser limits on total emissions, thus generating more electricity and greater economic profits. From Fig. 8(b), the optimal value has a non-decreasing monotonic trend with the environmental goal from 420 to 500, and the unachieved part increases with the increase of the social aspired goal. Thus, the realization value of the economic goal decreases due to the more stringent social impact.

In summary, when social and economic aspired goals are fixed, the environmental goal generally has a positive effect on achieving economic profit. However, when the environmental and economic goals are fixed, the social goal usually has a negative effect on the realization of the economic goal. Furthermore, optimal decisions, including location strategies, under different aspired goals are distinct. Hence, decision-makers need to set accurate aspired goals according to the practical problem's requirements.

7.3.2. Effects of biomass supply capacity

This section examines how biomass supply capacity influences the optimal value and the achievement of the economic goal. All parameters are kept constant as stated at the start of Section 7.3.

Fig. 9 illustrates that the optimal value is monotonically non-increasing with the biomass supply capacity. In such situations, the optimal value represents the unachieved part of the economic goal, as only the economic aspired goal is not always realized in calculating results. When the biomass supply capacity remains unchanged, the optimal value is approximately 0.007, implying that the unachieved part of the economic goal is approximately 0.007×10^8. As the biomass supply capacity gradually declines, the optimal value increases. In the extreme case, a 20% reduction in the biomass supply capacity leads to an optimal value of 3.243, indicating that the economic aspired goal value, which is 3.65×10^8, is just achieved by 0.407×10^8. Conversely, if the biomass supply increases by 5%, 10%, or 20%, the optimal value is always 0, implying that the economic goal is always achieved. It can be seen that sufficient biomass supply contributes to the achievement of economic aspired goal value.

In conclusion, biomass supply capacity has a crucial influence on the achievement of aspired goals. Setting appropriate aspired goals based on the available supply is essential for decision-makers to optimize the utilization of existing biomass.

7.3.3. Effects of biomass moisture contents

This section analyzes the effects of moisture contents of three types of biomass feedstock, including agricultural straws, forest residues, and livestock manures, on the optimal value and the achievement of the economic goal.

According to Fig. 10, subfigures (a), (b), and (c) show the relationships between the optimal value and the moisture contents of agricultural straws, forest residues, and livestock manures separately.

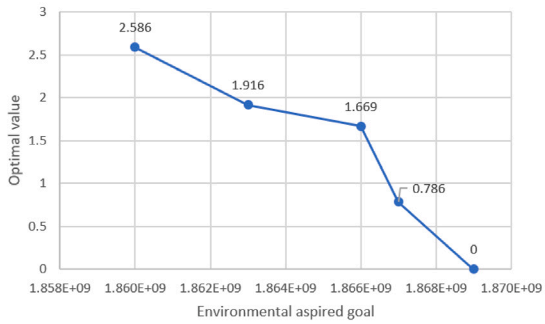

(a) Environmental aspired goal

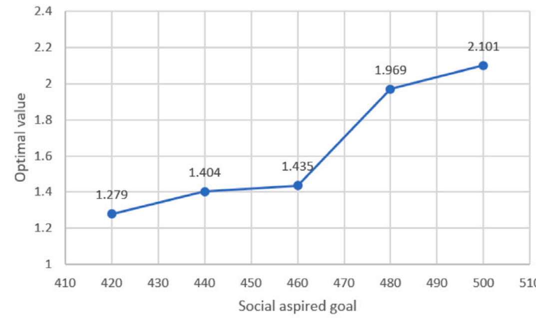

(b) Social aspired goal

Fig. 8. Optimal values under different environmental and social aspired goals.

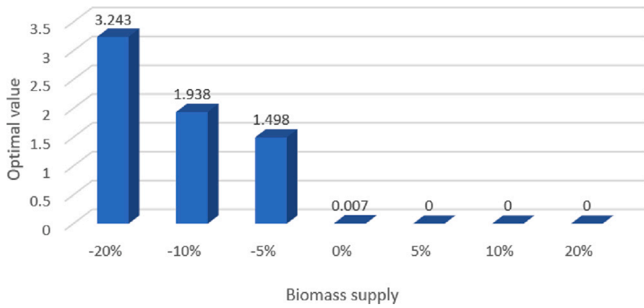

Fig. 9. Optimal values under different biomass supply capacity.

The three subfigures have the same trend of change, that is, with the increase in moisture content, the optimal value becomes larger, and the unachieved part of the economic goal also gets larger because it is still only the economic aspired goal has not been completely achieved in these cases. In other words, the realized value of the economic aspired goal decreases with the increase in the biomass moisture content. Taking Fig. 10(a) as an example, the optimal value increases sharply from 0.007 to 1.779 as the moisture content gradually increases from 0.2 to 0.226, which means the realized value of the economic aspired goal decreases from 3.643×10^8 to 1.871×10^8. It is possible that the reason for the smaller achieved value of the economic goal with a larger moisture content is due to the fact that higher moisture content in biomass results in less available biomass, which ultimately results in a decrease in the realized value of the economic goal.

Besides, in the case of different biomass moisture contents, the optimal network designs are not entirely the same. Therefore, decision-makers need to have comprehensive knowledge of parameters such as the moisture contents of various biomass feedstock in decision making.

7.3.4. Effects of biomass prices

It can be concluded that procurement cost is the largest contributor to total tactical cost in Section 7.1. Hereto, the effects of biomass prices on the optimal value and the economic aspired goal achievement are carried out.

Fig. 11 depicts the change of optimal value with respect to biomass prices. In general, the optimal value increases as the price of one of the biomass increases, however, there are exceptions. Note that the components in $(18.0, 15.0, 6.0)$ denotes the unit prices of agriculture straws, forest residues, and livestock matures in order, with others having similar meanings. In these cases, the environmental and social goals are still all achieved, while the economic goal is sensitive. Thus, the optimal value is a reflection of the unachieved portion of the economic goal. As shown in Fig. 11, the optimal value almost always increases and the corresponding achieved economic goal decreases as the price of one biomass increases. Note that the case where the price is $(18.0, 15.0, 7.0)$ is an exception. Compared with the cases of $(18.0, 15.0, 6.0)$ and $(18.0, 15.0, 6.5)$, although the price of livestock mature is higher, the optimal value becomes smaller. However, it does not take away from the fact that the increasing unit price generally results in an increased optimal value, thereby decreasing the realized economic profit. In addition, when the biomass price takes different values, the optimal network design decision is also different accordingly. As a result, it is necessary for the network designer to obtain a more precise biomass price in advance.

7.4. Management insights

According to computational results and analysis, we summarize several insights for decision-makers to incorporate some serviceable managements into the SBPSC network design problem.

- When multiple conflicting objectives in the SBPSC problem are not of equal importance to decision-makers, the proposed globalized robust goal programming model is a better alternative to obtain an optimal decision that meets the preference of decision-makers. By setting different priorities for different objectives, the realization sequence of multiple goals that is consistent with their importance degrees is ensured. In the context of the SBPSC problem, the environmental impact may be set as the top priority, the social objective the second, and the economic objective the last.
- Unit emissions and social scores are uncertain owing to the limited historical data available. In this case, using the nominal model to solve this problem will lead to a serious consequence, i.e., the solution obtained is not optimal or not even feasible when the data fluctuate. Compared with the robust goal programming model, it is shown that the proposed globalized robust goal programming model is less conservative. Therefore, the proposed model is preferable for decision-makers seeking a solution that can hedge against uncertainty without being overly conservative.
- The crucial issue in using the proposed model to make decisions is to determine the aspired goal values of multiple conflicting objectives in advance. Regarding this concern, the following suggestions are made for decision-makers. Firstly, each aspired goal value should be within its reasonable range, which can be referred to the payoff table obtained by solving the single objective model. Secondly, the environmental goal has a positive effect on the realization of the economic goal, while the social goal has a negative effect. Finally, to optimally utilize biomass resources, decision-makers need to adjust the size of the aspired goal value according to the biomass supply.

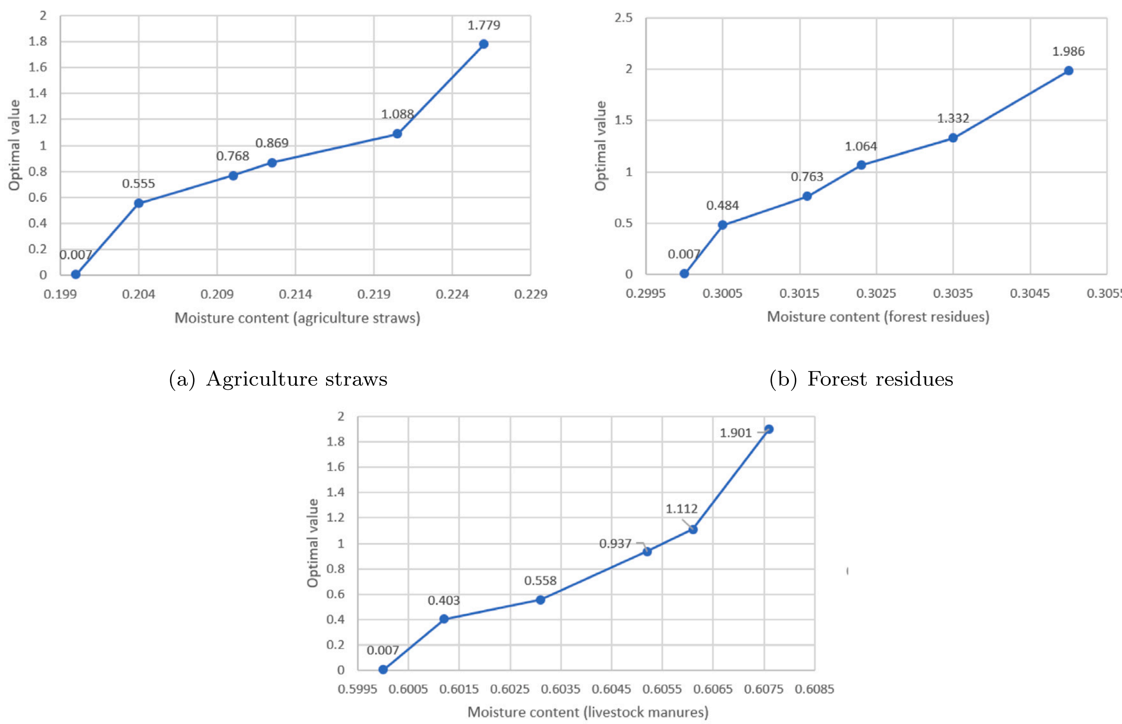

(a) Agriculture straws (b) Forest residues

(c) Livestock manures

Fig. 10. Optimal values under different moisture contents.

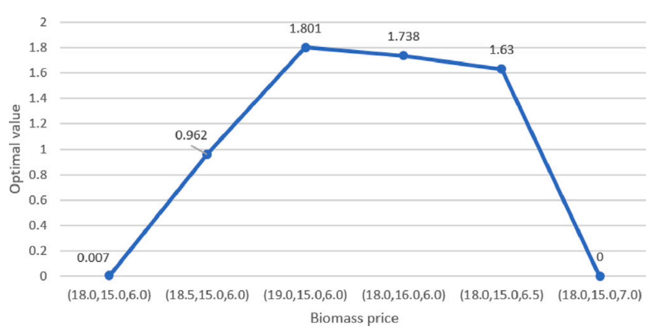

Fig. 11. Optimal values under different biomass prices.

- Another crucial problem in decision-making using the proposed model is determining the bounds of the inner and outer uncertainty sets. Due to limited data for uncertain parameters available, a box is selected as the outer uncertainty set, and the bound can be determined based on nominal values and support information. The inner budget set bound is chosen by decision-makers based on their conservatism attitudes or other presumable information of uncertain parameters. As a result, the inner–outer uncertainty set is not only less conservative but also more flexible in adjusting the robustness of the method against the conservatism level of the solution.
- The effects of some parameters on the optimal value and achievement of the economic goal are discussed in Sections 7.1 and 7.3. Specifically, the increase in some parameters, such as the biomass price, moisture content, and global sensitivity parameter, will result in an increase in the optimal value, a decrease in the achieved value of the economic goal, and a change in the optimal decision. Owing to the significant influence on optimal value and optimal decision, it is critical to implement accurate surveys of model parameters for decision-makers to obtain the preferred decision.

8. Conclusions

This study investigates a multi-objective SBPSC network design problem in uncertain environments, and proposes a novel globalized robust goal programming model. The proposed model in this study is distinct from existing related literature in that it considers the preferences of decision-makers for conflicting economic, environmental, and social objectives, as well as parameter uncertainty.

Given the growing emphasis on sustainable development, this study addresses the need to incorporate decision-makers' preferences for conflicting economic, environmental, and social objectives, as well as parameter uncertainty, into the proposed model. To achieve this, the environmental and social objectives are given higher priority than the economic objective. The uncertainty surrounding unit emissions and social scores has a significant impact on achieving economic goals. To account for parameter uncertainty, an inner–outer uncertainty set is introduced, which is used to formulate globalized robust environmental and social goal constraints. In the resulting globalized robust goal programming SBPSC model, the priority levels and aspired values of conflicting objectives are particularly important parameters and subject to the decision-makers' preference and judgement. Finally, the tractable equivalent form of the proposed SBPSC model is derived by converting environmental and social globalized robust goal constraints into finite systems of constraints by the Lagrange duality approach.

To demonstrate the effectiveness of the proposed approach, a case study about the design of a sustainable biomass-based power generation supply chain (SBPSC) network in Hubei Province is conducted. The main results are concluded as follows:

- The proposed globalized robust goal programming SBPSC model can hedge against parameter uncertainty and provide a robust network design decision that is immune to uncertainties.

- The proposed model is less conservative, and achieves a 42.5% greater realized economic goal than the robust goal programming model, on average, in the investigated situations.
- The economic objective is sensitive to parameter changes, while the environmental and social objectives can always achieve their aspired goals.
- Varying the aspired goal values for environmental, social, and economic objectives leads to different optimal values and decisions.
- Increasing the environmental aspired value leads to higher economic profits, while increasing the social aspired value results in a lower economic goal achievement.
- Optimal values and network design decisions change with exogenous parameters, including biomass supply capacity, biomass price, and moisture content.

The globalized robust optimization method is chosen to address parameter uncertainty owing to the lack of any distribution information for uncertain parameters. If partial distribution information based on historical data is available in practical situations, a distributionally robust optimization method would be a better choice for future research. Additionally, several other uncertain parameters in the design of the SBPSC network, including deterioration rate, conversion rate, biomass supply capacity, and costs, may influence the model's output and would be solved in our future research, where the biomass supply uncertainty could be coped with by incorporating different supply scenarios into the problem.

CRediT authorship contribution statement

Aixia Chen: Methodology, Data curation, Writing – original draft, Software. **Yankui Liu:** Methodology, Conceptualization, Validation, Writing – review & editing.

Declaration of competing interest

The authors declare that they have no conflicts of interest.

Data availability

No data was used for the research described in the article.

Acknowledgments

The authors are grateful to the Editor-in-Chief, Associate Editor, and anonymous reviewers for their insightful suggestions, which helped us to improve the manuscript significantly. This work was supported by the National Natural Science Foundation of China [grant number 61773150]; and the Operations Research and Management Innovation Team of Hebei University[grant number IT2023C02].

Appendix A. Proofs of main results

Proof of Theorem 1. Note that the constraint (16) is satisfied if and only if $H(\boldsymbol{V}) \le d_1^+ + g_1 - Emi_{tra}$ with

$$H(\boldsymbol{V}) = \sup_{\boldsymbol{\mu}\in\mathcal{U}_\mu} \left\{ \boldsymbol{\mu}^T\boldsymbol{V} - \min_{\boldsymbol{\mu}'\in\mathcal{U}'_\mu} \phi(\boldsymbol{\mu},\boldsymbol{\mu}') \right\},$$

where $\phi(\boldsymbol{\mu},\boldsymbol{\mu}')$ measures the distance between $\boldsymbol{\mu}$ and $\boldsymbol{\mu}'$. The distance function $\phi : \mathbb{R}^{GK}\times\mathbb{R}^{GK} \to \mathbb{R}$ is assumed to be nonnegative, closed, identical, and jointly convex. In this paper, the distance function takes the following form: $\phi(\boldsymbol{\mu},\boldsymbol{\mu}') = \alpha(\|\boldsymbol{\mu}-\boldsymbol{\mu}'\|_\infty)$, and $\alpha(\cdot)$ is convex, and nonnegative with $\alpha(0) = 0$.

Table B.1
Parameters about biomass.

	Price($/ton)	Holding cost in storage facility ($/ton)	Moisture content
Agricultural straws	18.0	3.0	0.2
Forest residues	15.0	1.0	0.3
Livestock manures	6.0	2.0	0.6

Let $h(\boldsymbol{\mu},\boldsymbol{V}) = \boldsymbol{\mu}^T\boldsymbol{V}$, then

$$H(\boldsymbol{V}) = \sup_{\boldsymbol{\mu}\in\mathcal{U}_\mu,\boldsymbol{\mu}'\in\mathcal{U}'_\mu,\boldsymbol{t},\boldsymbol{s}} \left\{ h(\boldsymbol{\mu},\boldsymbol{V}) - \phi(\boldsymbol{t},\boldsymbol{s}) | \boldsymbol{t}=\boldsymbol{\mu}, \boldsymbol{s}=\boldsymbol{\mu}' \right\}.$$

Slater's condition holds, hence by Lagrange duality it follows that

$$\begin{aligned} H(\boldsymbol{V}) &= \min_{\boldsymbol{w},\boldsymbol{z}} \sup_{\boldsymbol{\mu}\in\mathcal{U}_\mu,\boldsymbol{\mu}'\in\mathcal{U}'_\mu,\boldsymbol{t},\boldsymbol{s}} \left\{ h(\boldsymbol{\mu},\boldsymbol{V}) - \phi(\boldsymbol{t},\boldsymbol{s}) - \boldsymbol{w}^T(\boldsymbol{s}-\boldsymbol{\mu}') - \boldsymbol{z}^T(\boldsymbol{t}-\boldsymbol{\mu}) \right\} \\ &= \min_{\boldsymbol{w},\boldsymbol{z}} \left\{ \sup_{\boldsymbol{\mu}\in\mathcal{U}_\mu} \{h(\boldsymbol{\mu},\boldsymbol{V}) + \boldsymbol{z}^T\boldsymbol{\mu}\} + \sup_{\boldsymbol{t},\boldsymbol{s}}\{-\phi(\boldsymbol{t},\boldsymbol{s}) - \boldsymbol{z}^T\boldsymbol{t} - \boldsymbol{w}^T\boldsymbol{s}\} \right. \\ &\quad \left. + \sup_{\boldsymbol{\mu}'\in\mathcal{U}'_\mu} \{\boldsymbol{w}^T\boldsymbol{\mu}'\} \right\}. \end{aligned}$$

Denote $h_1(\boldsymbol{z},\boldsymbol{V}) = \sup_{\boldsymbol{\mu}\in\mathcal{U}_\mu}\{h(\boldsymbol{\mu},\boldsymbol{V})+\boldsymbol{z}^T\boldsymbol{\mu}\}$, $h_2(\boldsymbol{w},\boldsymbol{z}) = \sup_{\boldsymbol{t},\boldsymbol{s}}\{-\phi(\boldsymbol{t},\boldsymbol{s}) - \boldsymbol{z}^T\boldsymbol{t} - \boldsymbol{w}^T\boldsymbol{s}\}$, $h_3(\boldsymbol{w}) = \sup_{\boldsymbol{\mu}'\in\mathcal{U}'_\mu}\{\boldsymbol{w}^T\boldsymbol{\mu}'\}$, then $H(\boldsymbol{V})$ is simplified as follows:

$$H(\boldsymbol{V}) = \min_{\boldsymbol{w},\boldsymbol{z}} \left\{ h_1(\boldsymbol{z},\boldsymbol{V}) + h_2(\boldsymbol{w},\boldsymbol{z}) + h_3(\boldsymbol{w}) \right\}. \tag{A.1}$$

Based on the definition of the indicator function $\delta(\boldsymbol{\mu}|\mathcal{U}_\mu)$, and Fenchel duality, the first part is rewritten as follows:

$$h_1(\boldsymbol{z},\boldsymbol{V}) = \min_{\boldsymbol{v}}\{\delta^*(\boldsymbol{v}|\mathcal{U}_\mu) - [h(\boldsymbol{v},\boldsymbol{V}) + \boldsymbol{z}^T\boldsymbol{v}]_*\},$$

and by the relationship between $\mathcal{U}_\mu$ and $\mathcal{Z}_\mu$, it is derived $h_1(\boldsymbol{z},\boldsymbol{V}) = \min_{\boldsymbol{v}}\{(\boldsymbol{\mu}^0)^T\boldsymbol{v} + \delta^*(\boldsymbol{A}^T\boldsymbol{v}|\mathcal{Z}_\mu) - h_*(\boldsymbol{v}-\boldsymbol{z},\boldsymbol{V})\}$.

The second part simplifies as follows:

$$h_2(\boldsymbol{w},\boldsymbol{z}) = \sup_{\boldsymbol{t},\boldsymbol{s}}\{-\phi(\boldsymbol{t},\boldsymbol{s}) - \boldsymbol{z}^T\boldsymbol{t} - \boldsymbol{w}^T\boldsymbol{s}\} = \phi^{**}(-\boldsymbol{z},-\boldsymbol{w}).$$

And the third part simplifies to

$$h_3(\boldsymbol{w}) = \sup_{\boldsymbol{\mu}'\in\mathcal{U}'_\mu}\{\boldsymbol{w}^T\boldsymbol{\mu}'\} = \delta^*(\boldsymbol{w}|\mathcal{U}'_\mu) = (\boldsymbol{\mu}^0)^T\boldsymbol{w} + \delta^*(\boldsymbol{A}^T\boldsymbol{w}|\mathcal{Z}'_\mu).$$

After substituting these formulas in (A.1), the constraint (16) is equivalently formulated as follows:

$$\begin{aligned} &\min_{\boldsymbol{w},\boldsymbol{z}}\{\min_{\boldsymbol{v}}\{(\boldsymbol{\mu}^0)^T\boldsymbol{v} + \delta^*(\boldsymbol{A}^T\boldsymbol{v}|\mathcal{Z}_\mu) - h_*(\boldsymbol{v}-\boldsymbol{z},\boldsymbol{V})\} \\ &\quad + \phi^{**}(-\boldsymbol{z},-\boldsymbol{w}) + (\boldsymbol{\mu}^0)^T\boldsymbol{w} + \delta^*(\boldsymbol{A}^T\boldsymbol{w}|\mathcal{Z}'_\mu)\} \le d_1^+ + g_1 - Emi_{tra}. \end{aligned}$$

Consequently, $H(\boldsymbol{V}) \le d_1^+ + g_1 - Emi_{tra}$ when and only when there are $\boldsymbol{w},\boldsymbol{z}$, and $\boldsymbol{v}$ such that

$$\begin{aligned} &(\boldsymbol{\mu}^0)^T\boldsymbol{v} + \delta^*(\boldsymbol{A}^T\boldsymbol{v}|\mathcal{Z}_\mu) - h_*(\boldsymbol{v}-\boldsymbol{z},\boldsymbol{V}) + \phi^{**}(-\boldsymbol{z},-\boldsymbol{w}) \\ &\quad + (\boldsymbol{\mu}^0)^T\boldsymbol{w} + \delta^*(\boldsymbol{A}^T\boldsymbol{w}|\mathcal{Z}'_\mu) \le d_1^+ + g_1 - Emi_{tra}. \end{aligned} \tag{A.2}$$

By the definition of the convex conjugate function, $\phi^{**}(-\boldsymbol{z},-\boldsymbol{w})$ is finite only if $\boldsymbol{z} = -\boldsymbol{w}$. And because $\phi(\boldsymbol{\mu},\boldsymbol{\mu}') = \alpha(\|\boldsymbol{\mu}-\boldsymbol{\mu}'\|_\infty)$ with $\alpha(x) = \theta_\mu x(x \ge 0)$, then $\phi^{**}(\boldsymbol{w},-\boldsymbol{w}) = 0$ only if $\|\boldsymbol{w}\|_1 \le \theta_\mu$.

Note that $h_*(\boldsymbol{v}-\boldsymbol{z},\boldsymbol{V}) = h_*(\boldsymbol{v}+\boldsymbol{w},\boldsymbol{V})$ due to $\boldsymbol{z} = -\boldsymbol{w}$. And because $h(\boldsymbol{\mu},\boldsymbol{V}) = \boldsymbol{\mu}^T\boldsymbol{V}$, we have

$$h_*(\boldsymbol{v}+\boldsymbol{w},\boldsymbol{V}) = \min_{\boldsymbol{\mu}}\{\boldsymbol{\mu}^T(\boldsymbol{v}+\boldsymbol{w}) - \boldsymbol{\mu}^T\boldsymbol{V}\} = \begin{cases} 0, if & \boldsymbol{v}+\boldsymbol{w} = \boldsymbol{V} \\ -\infty, if & \boldsymbol{v}+\boldsymbol{w} \ne \boldsymbol{V} \end{cases}$$

Based on the uncertainty sets with perturbation set $(\mathcal{Z}'_\mu, \mathcal{Z}_\mu)$, as indicated in Section 5.2, one gets

$$\delta^*(\boldsymbol{A}^T\boldsymbol{v}|\mathcal{Z}_\mu) = \max_{\boldsymbol{\zeta}\in\mathcal{Z}_\mu}\{\boldsymbol{\zeta}^T(\boldsymbol{A}^T\boldsymbol{v})\} = \tau_\mu\|\boldsymbol{A}^T\boldsymbol{v}\|_1,$$

Table B.2
The distances between potential storage facilities and potential power plants (km).

Potential storage facilities	Potential power plants											
	P_1	P_2	P_3	P_4	P_5	P_6	P_7	P_8	P_9	P_{10}	P_{11}	P_{12}
P_1	0	62	248	173	159	270	98	232	86	100	276	189
P_2	62	0	306	236	219	315	87	258	135	154	337	250
P_3	248	306	0	132	91	100	333	363	173	226	61	170
P_4	173	236	132	0	72	214	232	231	141	108	124	43
P_5	159	219	91	72	0	149	242	287	94	139	118	114
P_6	270	315	100	214	149	0	366	435	184	283	159	255
P_7	98	87	333	232	242	366	0	179	183	127	350	230
P_8	232	258	363	231	287	435	179	0	287	157	348	199
P_9	86	135	173	141	94	184	183	287	0	131	211	174
P_{10}	100	154	226	108	139	283	127	157	131	0	231	104
P_{11}	276	337	61	124	118	159	350	348	211	231	0	150
P_{12}	189	250	170	43	114	255	230	199	174	104	150	0

Table B.3
The distances between biomass suppliers and potential power plants (km).

Biomass suppliers	Potential storage facilities or power plants											
	P_1	P_2	P_3	P_4	P_5	P_6	P_7	P_8	P_9	P_{10}	P_{11}	P_{12}
S_1	251	211	493	389	402	521	160	256	337	281	509	381
S_2	224	224	418	293	331	473	137	104	301	193	417	271
S_3	108	99	340	235	248	375	12	170	193	128	354	231
S_4	227	255	355	223	279	427	178	8	280	150	340	190
S_5	199	239	300	167	226	375	175	64	239	108	284	134
S_6	208	257	259	129	196	342	208	115	228	108	237	90
S_7	170	201	315	186	233	380	129	62	225	98	308	161
S_8	158	200	277	146	197	345	142	90	200	69	268	121
S_9	100	154	226	108	139	283	127	157	131	0	231	104
S_{10}	83	125	259	147	169	308	87	151	140	40	268	144
S_{11}	77	95	296	191	205	335	41	164	156	86	310	189
S_{12}	53	113	219	125	127	259	115	200	88	51	237	137
S_{13}	84	56	329	239	239	353	34	212	169	140	352	243
S_{14}	55	51	299	210	209	325	45	207	141	114	322	216
S_{15}	8	60	254	176	165	278	90	226	94	98	281	190
S_{16}	27	44	262	197	176	273	106	255	92	128	294	215
S_{17}	58	118	191	125	102	219	148	244	43	90	219	150
S_{18}	76	109	209	178	134	206	173	300	40	150	250	209
S_{19}	199	257	205	77	148	291	225	169	198	104	181	35
S_{20}	206	267	148	38	106	238	255	226	179	128	123	28
S_{21}	111	173	173	64	86	232	170	203	102	53	181	79
S_{22}	140	202	128	42	44	193	211	243	99	98	140	79
S_{23}	152	212	99	69	8	155	235	280	89	131	125	111
S_{24}	92	154	163	87	72	207	170	235	62	79	185	114
S_{25}	109	164	141	110	59	167	201	281	35	124	177	146
S_{26}	123	164	161	164	102	151	222	328	42	171	209	201
S_{27}	165	206	137	174	104	110	264	361	81	204	192	215
S_{28}	186	222	144	195	123	99	284	384	103	227	202	236
S_{29}	223	264	120	201	129	56	321	407	137	251	181	243
S_{30}	284	331	95	217	155	20	380	442	199	293	150	257
S_{31}	320	368	110	240	184	56	414	468	234	323	155	279
S_{32}	258	308	60	180	120	40	351	406	173	258	119	220
S_{33}	301	353	71	203	154	66	392	433	218	292	113	240
S_{34}	193	248	60	117	50	99	283	337	114	188	110	159
S_{35}	284	339	43	175	131	82	373	406	204	268	84	212
S_{36}	208	269	55	78	50	142	287	309	143	174	68	116
S_{37}	246	305	24	115	87	124	327	346	176	214	42	150
S_{38}	301	359	53	171	142	121	384	400	226	272	57	202
S_{39}	247	308	77	86	96	176	316	309	190	194	39	110
S_{40}	276	337	61	124	118	159	350	348	211	231	0	150

Table B.4
Electricity generation rate of various technologies.

	Agricultural straws	Forest residues	Livestock manures
LFGRS	410	478	398
Incinerator	695	787	648
AD	591	688	538
ATT	758	860	708

and

$$\delta^*(\boldsymbol{A}^T\boldsymbol{w}|\mathcal{Z}'_\mu) = \max_{\zeta\in\mathcal{Z}'_\mu}\{\boldsymbol{\zeta}^T(\boldsymbol{A}^T\boldsymbol{w})\}$$

$$= \Gamma_\mu\|\boldsymbol{e}\|_\infty + \tau'_\mu\|\boldsymbol{f}\|_1 \qquad \text{with } \boldsymbol{e}+\boldsymbol{f} = \boldsymbol{A}^T\boldsymbol{w}.$$

Finally, substitute these formulas into (A.2), then (A.2) is crystallized as the following system,

$$\begin{cases} (\boldsymbol{\mu}^0)^T\boldsymbol{V} + \Gamma_\mu\|\boldsymbol{e}\|_\infty + \tau'_\mu\|\boldsymbol{f}\|_1 + \tau_\mu\|\boldsymbol{A}^T\boldsymbol{v}\|_1 \le d_1^+ + g_1 - Emi_{tra} \\ \boldsymbol{e}+\boldsymbol{f} = \boldsymbol{A}^T\boldsymbol{w} \\ \boldsymbol{v}+\boldsymbol{w} = \boldsymbol{V} \\ \|\boldsymbol{w}\|_1 \le \theta_\mu \end{cases}$$

The proof of theorem is complete. □

Table B.5
Fixed costs and final social scores of biomass power production technologies.

Technology	LFGRS			Incinerator			AD			ATT		
Capacity	1	2	3	1	2	3	1	2	3	1	2	3
Annualized fixed cost (million$)	3.6	5.5	6.0	20.1	27.3	30	29.5	36.5	38.1	31.5	42.8	45.6
Final social score ($\sum_c \boldsymbol{w}_c \rho_{ckr}$)	78	82	88	55	59	64	97	105	110	81	87	94

Table B.6
Monthly electricity consumption (MWh).

	Jan.	Feb.	Mar.	Apr.	May	Jun.	Jul.	Aug.	Sept.	Oct.	Nov.	Dec.
Agriculture	15547	15436	17061	17967	17210	18721	19755	19101	17992	17719	16856	15835
Industry	556389	560163	565971	557998	565123	551952	564240	569001	553067	551908	555420	558527
Transport	150229	155599	152748	145480	155745	143890	149010	148175	142196	148551	148331	147383
Living	173880	179011	162128	159399	158942	180999	192906	199464	153804	154165	177463	177933

Table B.7
Unit emission amounts of various technologies (kg/ton).

	CO_2	NO_x	Heavy metals	VOC
LFGRS	300	0.68	0.0000374	0.0064
Incinerator	1000	1.6	0.01253	0.008
AD	227	0.188	0.0027012	2.1
ATT	438	0.78	0.0041359	0.011

Proof of Theorem 2. Constraint (19) is equivalently written as $G(\boldsymbol{X}) \le d_2^- - g_2$ with

$$G(\boldsymbol{X}) = \sup_{\rho \in \mathcal{U}_\rho} \{-\boldsymbol{\rho}^T \boldsymbol{X} - \min_{\rho' \in \mathcal{U}'_\rho} \phi(\rho, \rho')\},$$

where $\rho = (\sum_{g\in[G]} \rho_{gkr})_{k\in[K],r\in[R]}$, and $\boldsymbol{X} = (\sum_{j\in[J]} \sum_{m\in[M]} X_{jkmr})_{k\in[K],r\in[R]}$. The value $\phi(\boldsymbol{\rho}, \boldsymbol{\rho}')$ measures the distance between $\boldsymbol{\rho}$ and $\boldsymbol{\rho}'$. Here, the distance function is $\phi(\rho, \rho') = \alpha(\|\boldsymbol{\rho} - \boldsymbol{\rho}'\|_\infty)$, and $\alpha(\cdot)$ is convex, and nonnegative with $\alpha(0) = 0$.

Let $g(\rho, \boldsymbol{X}) = -\boldsymbol{\rho}^T \boldsymbol{X}$, based on Lagrange duality and Slater's condition, after introducing auxiliary variables $\boldsymbol{u}, \boldsymbol{q}$, and dual variables $\boldsymbol{\sigma}, \boldsymbol{y}$, one has

$$G(\boldsymbol{X}) = \min_{\boldsymbol{\sigma},\boldsymbol{y}} \left\{ \sup_{\rho \in \mathcal{U}_\rho} \{g(\rho, \boldsymbol{X}) + \boldsymbol{y}^T(-\rho)\} + \sup_{\boldsymbol{u},\boldsymbol{q}} \{-\phi(\boldsymbol{u}, \boldsymbol{q}) - \boldsymbol{y}^T \boldsymbol{u} - \boldsymbol{\sigma}^T \boldsymbol{q}\} \right.$$
$$\left. + \sup_{\rho' \in \mathcal{U}'_\rho} \{\boldsymbol{\sigma}^T(-\boldsymbol{\rho}')\} \right\}.$$

For the sake of derivation, denote

$$g_1(\boldsymbol{y}, \boldsymbol{X}) = \sup_{\rho \in \mathcal{U}_\rho} \{g(\rho, \boldsymbol{X}) + \boldsymbol{y}^T(-\rho)\},$$
$$g_2(\boldsymbol{\sigma}, \boldsymbol{y}) = \sup_{\boldsymbol{u},\boldsymbol{q}} \{-\phi(\boldsymbol{u}, \boldsymbol{q}) - \boldsymbol{y}^T \boldsymbol{u} - \boldsymbol{\sigma}^T \boldsymbol{q}\},$$
$$g_3(\boldsymbol{\sigma}) = \sup_{\rho' \in \mathcal{U}'_\rho} \{\boldsymbol{\sigma}^T(-\boldsymbol{\rho}')\}.$$

The first term is calculated as follows:

$$g_1(\boldsymbol{y}, \boldsymbol{X}) = \min_{\boldsymbol{\varphi}} \{\delta^*(-\boldsymbol{\varphi}|\mathcal{U}_\rho) - [g(\boldsymbol{\varphi}, \boldsymbol{X}) + \boldsymbol{y}^T(-\boldsymbol{\varphi})]_*\}$$
$$= \min_{\boldsymbol{\varphi}} \{(-\rho^0)^T \boldsymbol{\varphi} + \delta^*(-\boldsymbol{B}^T \boldsymbol{\varphi}|\mathcal{Z}_\rho) - g_*(\boldsymbol{\varphi} - \boldsymbol{y}, \boldsymbol{X})\}$$

The second term simplifies to $g_2(\boldsymbol{\sigma}, \boldsymbol{y}) = \phi^{**}(-\boldsymbol{\sigma}, -\boldsymbol{y})$.
Finally, the third term is as follows:

$$g_3(\boldsymbol{\sigma}) = \delta^*(-\rho'|\mathcal{U}'_\rho) = (-\rho^0)^T \boldsymbol{\sigma} + \delta^*(-\boldsymbol{B}^T \boldsymbol{\sigma}|\mathcal{Z}'_\rho).$$

Therefore, the expression $G(\boldsymbol{X}) \le d_2^- - g_2$ is rewritten as

$$\min_{\boldsymbol{\sigma},\boldsymbol{y}} \left\{ \min_{\boldsymbol{\varphi}} \{(-\rho^0)^T \boldsymbol{\varphi} + \delta^*(-\boldsymbol{B}^T \boldsymbol{\varphi}|\mathcal{Z}_\rho) - g_*(\boldsymbol{\varphi} - \boldsymbol{y}, \boldsymbol{X})\} \right.$$
$$\left. + \ \phi^{**}(-\boldsymbol{\sigma}, -\boldsymbol{y}) + (-\rho^0)^T \boldsymbol{\sigma} + \delta^*(-\boldsymbol{B}^T \boldsymbol{\sigma}|\mathcal{Z}'_\rho) \right\} \le d_2^- - g_2,$$

which holds true when and only when there are $\boldsymbol{\varphi}, \boldsymbol{\sigma}, \boldsymbol{y}$ such that

$$(-\rho^0)^T \boldsymbol{\varphi} + \delta^*(-\boldsymbol{B}^T \boldsymbol{\varphi}|\mathcal{Z}_\rho) - g_*(\boldsymbol{\varphi} - \boldsymbol{y}, \boldsymbol{X}) + \phi^{**}(-\boldsymbol{\sigma}, -\boldsymbol{y})$$
$$+ \ (-\rho^0)^T \boldsymbol{\sigma} + \delta^*(-\boldsymbol{B}^T \boldsymbol{\sigma}|\mathcal{Z}'_\rho) \le d_2^- - g_2, \tag{A.3}$$

According to the definition of convex conjugate, $\phi^{**}(-\boldsymbol{\sigma}, -\boldsymbol{y})$ is a finite value only if $\boldsymbol{\sigma} = \boldsymbol{y}$. Furthermore, $\phi^{**}(-\boldsymbol{\sigma}, \boldsymbol{\sigma}) = 0$ when $\|\boldsymbol{\sigma}\|_1 \le \theta_\rho$. In addition, $g_*(\boldsymbol{\varphi} - \boldsymbol{y}, \boldsymbol{X}) = g_*(\boldsymbol{\varphi} + \boldsymbol{\sigma}, \boldsymbol{X}) = 0$ only if $\boldsymbol{\varphi} + \boldsymbol{\sigma} = \boldsymbol{X}$.

Based on the perturbation sets $(\mathcal{Z}'_\rho, \mathcal{Z}_\rho)$, one has

$$\delta^*(-\boldsymbol{B}^T \boldsymbol{\varphi}|\mathcal{Z}_\rho) = \max_{\zeta \in \mathcal{Z}_\rho} \{\boldsymbol{\zeta}^T(-\boldsymbol{B}^T \boldsymbol{\varphi})\} = \tau_\rho \|\boldsymbol{B}^T \boldsymbol{\varphi}\|_1,$$

and

$$\delta^*(-\boldsymbol{B}^T \boldsymbol{\sigma}|\mathcal{Z}'_\rho) = \max_{\zeta \in \mathcal{Z}'_\rho} \{\boldsymbol{\zeta}^T(-\boldsymbol{B}^T \boldsymbol{\sigma})\} = \Gamma_\rho \|\boldsymbol{c}\|_\infty + \tau'_\rho \|\boldsymbol{d}\|_1$$

with $\boldsymbol{c} + \boldsymbol{d} = \boldsymbol{B}^T \boldsymbol{\sigma}$.

As a consequence, substitute these expressions into total-formula (2), then total-formula (2) is formed as the following system,

$$\begin{cases} (\rho^0)^T \boldsymbol{X} - \Gamma_\rho \|\boldsymbol{c}\|_\infty - \tau'_\rho \|\boldsymbol{d}\|_1 - \tau_\rho \|\boldsymbol{B}^T \boldsymbol{\varphi}\|_1 + d_2^- \ge g_2 \\ \boldsymbol{c} + \boldsymbol{d} = \boldsymbol{B}^T \boldsymbol{\sigma} \\ \boldsymbol{\varphi} + \boldsymbol{\sigma} = \boldsymbol{X} \\ \|\boldsymbol{\sigma}\|_1 \le \theta_\rho \end{cases}$$

The proof of theorem is complete. □

Appendix B. Experimental data

See Tables B.1–B.7.

Appendix C. Checking the uncertainty in influencing parameters

To check the uncertainty in the influencing parameters and identify the most influential parameters in the SBPSC problem, the LSA approach (Ahmadvand and Sowlati, 2022) is used to analyze the deterministic model, i.e., the nominal goal programming model in Section 7.2.

According to the calculation results of Section 7.2, the optimal value of the deterministic model is 0, which indicates that the aspired goal values of environmental, social, and economic objectives are all achieved. However, owing to the changeable external environment, some parameters are prone to vary their values, such as social score, unit emission, deterioration rate, conversion rate, moisture content, unit purchasing cost, unit operating cost, unit holding cost, electricity demand, and biomass supply capacity, and therefore the parameter uncertainty should be addressed to avoid the infeasibility and inefficiency. The sensitivity of optimal value to ±50% change of these uncertain parameters is examined using the LSA approach, in which only one parameter is varied at a time, and others are set to be their nominal values (Ahmadvand and Sowlati, 2022), as shown in Table C.1.

From Table C.1, all considered influencing parameters have some effects on the deterministic model's optimal value that reflects the unrealized part of the economic goal as environmental and social goals are

Table C.1
The sensitivity of optimal value to ±50% change in influencing parameters.

Uncertainty parameters	−50%	+50%	Uncertainty parameters	−50%	+50%
Social scores	3.048	1.432	Unit purchasing cost	0.000	1.390
Unit emissions	0.000	1.566	Unit operating cost	0.000	0.778
Deterioration rate	0.762	0.000	Unit holding cost	1.491	0.000
Conversion rate	Infeasible	0.000	Electricity demand	1.231	Infeasible
Moisture content	0.000	Infeasible	Biomass supply capacity	Infeasible	0.000

always achieved in these cases. The social score is the most influencing parameter as a 50% decrease in social score results in an optimal value of 3.048; while a 50% increase eventuates an optimal value of 1.432. Next, the optimal value is most sensitive to unit emission as a 50% increase in unit emission leads to an optimal value of 1.566. When unit emission has decreased by 50%, the optimal value is still 0, indicating complete achievements of environmental, social, and economic goals; with other optimal values of 0 having similar meanings. With the existing supply available, when a 50% decrease in the conversion rate occurs, there is no feasible solution since the electricity demand will not be satisfied. Similarly, other "infeasible" situations are generally caused indirectly by inadequate supply or unmet demand. Note that unit costs of purchasing, operating, and holding, biomass supply, electricity demand, deterioration rate, conversion rate, and moisture content have relatively less influence. In the context of sustainability, this study primarily considers the uncertainty of social score and unit emission in the SBPSC problem.

References

Aboytes-Ojeda, M., Castillo-Villar, K.K., Cardona-Valdés, Y., 2022. Bi-objective stochastic model for the design of biofuel supply chains incorporating risk. Expert Syst. Appl. 202, 117285. http://dx.doi.org/10.1016/j.eswa.2022.117285.

Acquaye, A., Feng, K., Oppon, E., Salhi, S., Ibn-Mohammed, T., Genovese, A., Hubacek, K., 2017. Measuring the environmental sustainability performance of global supply chains: A multi-regional input–output analysis for carbon, sulphur oxide and water footprints. J. Environ. Manag. 187, 571–585. http://dx.doi.org/10.1016/j.jenvman.2016.10.059.

Ahmadvand, S., Sowlati, T., 2022. A robust optimization model for tactical planning of the forest-based biomass supply chain for syngas production. Comput. Chem. Eng 159, 107693. http://dx.doi.org/10.1016/j.compchemeng.2022.107693.

Akhtari, S., Sowlati, T., 2020. Hybrid optimization-simulation for integrated planning of bioenergy and biofuel supply chains. Appl. Energy 259, 114124. http://dx.doi.org/10.1016/j.apenergy.2019.114124.

Almeida, C.M.V.B., Madureira, M.A., Bonilla, S.H., Giannetti, B.F., 2013. Assessing the replacement of lead in solders: effects on resource use and human health. J. Clean. Prod. 47, 457–464. http://dx.doi.org/10.1016/j.jclepro.2012.08.002.

Andrews, E.S., 2009. Guidelines for social life cycle assessment of products: social and socio-economic LCA guidelines complementing environmental LCA and life cycle costing, contributing to the full assessment of goods and services within the context of sustainable development. UNEP/Earthprint.

Aranguren, M.F., Castillo-Villar, K.K., 2022. Bi-objective stochastic model for the design of large-scale carbon footprint conscious co-firing biomass supply chains. Comput. Ind. Eng. 171, 108352. http://dx.doi.org/10.1016/j.cie.2022.108352.

Aranguren, M., Castillo-Villar, K.K., Aboytes-Ojeda, M., 2021. A two-stage stochastic model for co-firing biomass supply chain networks. J. Clean. Prod. 319, 128582. http://dx.doi.org/10.1016/j.jclepro.2021.128582.

Barbosa-Póvoa, A.P., da Silva, C., Carvalho, A., 2018. Opportunities and challenges in sustainable supply chain: An operations research perspective. Eur. J. Oper. Res. 268 (2), 399–431. http://dx.doi.org/10.1016/j.ejor.2017.10.036.

Basile, F., Pilotti, L., Ugolini, M., Lozza, G., Manzolini, G., 2022. Supply chain optimization and GHG emissions in biofuel production from forestry residues in Sweden. Renew. Energy 196, 405–421. http://dx.doi.org/10.1016/j.renene.2022.06.095.

Ben-Tal, A., Brekelmans, R., Den Hertog, D., Vial, J.P., 2017. Globalized robust optimization for nonlinear uncertain inequalities. INFORMS J. Comput. 29 (2), 350–366. http://dx.doi.org/10.1287/ijoc.2016.0735.

Ben-Tal, A., El Ghaoui, L., Nemirovski, A., 2009. Robust Optimization. Princeton University Press.

BP, B., 2022. Statistical review of world energy 2022.

Cambero, C., Sowlati, T., 2014. Assessment and optimization of forest biomass supply chains from economic, social and environmental perspectives–a review of literature. Renew. Sustain. Energy Rev. 36, 62–73. http://dx.doi.org/10.1016/j.rser.2014.04.041.

Cao, C., Liu, Y., Tang, O., Gao, X., 2021. A fuzzy bi-level optimization model for multi-period post-disaster relief distribution in sustainable humanitarian supply chains. Int. J. Prod. Econ. 235, 108081. http://dx.doi.org/10.1016/j.ijpe.2021.108081.

Charnes, A., Cooper, W.W., 1961. Management Models and Industrial Applications of Linear Programming. John Wiley, New York.

Delkhosh, F., Sadjadi, S.J., 2020. A robust optimization model for a biofuel supply chain under demand uncertainty. Int. J. Energy Environ. E 11 (2), 229–245. http://dx.doi.org/10.1007/s40095-019-00329-w.

Díaz-Trujillo, L.A., Fuentes-Cortés, L.F., Nápoles-Rivera, F., 2020. Economic and environmental optimization for a biogas supply chain: A CVaR approach applied to uncertainty of biomass and biogas demand. Comput. Chem. Eng. 141, 107018. http://dx.doi.org/10.1016/j.compchemeng.2020.107018.

Evans, A., Strezov, V., Evans, T.J., 2010. Sustainability considerations for electricity generation from biomass. Renew. Sustain. Energy Rev. 14 (5), 1419–1427. http://dx.doi.org/10.1016/j.rser.2010.01.010.

Fattahi, M., Govindan, K., Farhadkhani, M., 2021. Sustainable supply chain planning for biomass-based power generation with environmental risk and supply uncertainty considerations: a real-life case study. Int. J. Prod. Res. 59 (10), 3084–3108. http://dx.doi.org/10.1080/00207543.2020.1746427.

Feng, Y., Chen, Y., Liu, Y., 2022. Optimising two-stage robust supplier selection and order allocation problem under risk-averse criterion. Int. J. Prod. Res. 1–25. http://dx.doi.org/10.1080/00207543.2022.2127963.

Fernández-Puratich, H., Rebolledo-Leiva, R., Hernández, D., Gómez-Lagos, J.E., Armengot-Carbo, B., Oliver-Villanueva, J.V., 2021. Bi-objective optimization of multiple agro-industrial wastes supply to a cogeneration system promoting local circular bioeconomy. Appl. Energy 300, 117333. http://dx.doi.org/10.1016/j.apenergy.2021.117333.

García-Velásquez, C., Leduc, S., Van Der Meer, Y., 2022. Design of biobased supply chains on a life cycle basis: A bi-objective optimization model and a case study of biobased polyethylene terephthalate (PET). Sustain. Prod. Consump. 30, 706–719. http://dx.doi.org/10.1016/j.spc.2022.01.003.

Ghaderi, H., Moini, A., Pishvaee, M.S., 2018. A multi-objective robust possibilistic programming approach to sustainable switchgrass-based bioethanol supply chain network design. J. Clean. Prod. 179, 368–406. http://dx.doi.org/10.1016/j.jclepro.2017.12.218.

Gilani, H., Sahebi, H., Oliveira, F., 2020. Sustainable sugarcane-to-bioethanol supply chain network design: A robust possibilistic programming model. Appl. Energy 278, 115653. http://dx.doi.org/10.1016/j.apenergy.2020.115653.

Global Bioenergy Statistics, 2021. World bioenergy association.

Gumte, K., Pantula, P.D., Miriyala, S.S., Mitra, K., 2021a. Achieving wealth from bio-waste in a nationwide supply chain setup under uncertain environment through data driven robust optimization approach. J. Clean. Prod 291, 125702. http://dx.doi.org/10.1016/j.jclepro.2020.125702.

Gumte, K.M., Pantula, P.D., Miriyala, S.S., Mitra, K., 2021b. Data driven robust optimization for handling uncertainty in supply chain planning models. Chem. Eng. Sci. 246, 116889. http://dx.doi.org/10.1016/j.ces.2021.116889.

Guo, C., Hu, H., Wang, S., Rodriguez, L.F., Ting, K.C., Lin, T., 2022. Multiperiod stochastic programming for biomass supply chain design under spatiotemporal variability of feedstock supply. Renew. Energy 186, 378–393. http://dx.doi.org/10.1016/j.renene.2021.12.144.

Habib, M.S., Tayyab, M., Zahoor, S., Sarkar, B., 2020. Management of animal fat-based biodiesel supply chain under the paradigm of sustainability. Energy Convers. Manag. 225, 113345. http://dx.doi.org/10.1016/j.enconman.2020.113345.

Hombach, L.E., Cambero, C., Sowlati, T., Walther, G., 2016. Optimal design of supply chains for second generation biofuels incorporating European biofuel regulations. J. Clean. Prod. 133, 565–575. http://dx.doi.org/10.1016/j.jclepro.2016.05.107.

Inapakurthi, R.K., Pantula, P.D., Miriyala, S.S., Mitra, K., 2020. Data driven robust optimization of grinding process under uncertainty. Mater. Manuf. Process. 35 (16), 1870–1876. http://dx.doi.org/10.1080/10426914.2020.1802042.

Intergovernmental Panel on Climate Change, 2018. Global Warming of 1.5°C: An IPCC Special Report on the Impacts of Global Warming of 1.5°C above Pre-Industrial Levels and Related Global Greenhouse Gas Emission Pathways, in the Context of Strengthening the Global Response To the Threat of Climate Change, Sustainable Development, and Efforts To Eradicate Poverty. Intergovernmental Panel on Climate Change.

Karimi, H., Eksioğlu, S.D., Carbajales-Dale, M., 2021. A biobjective chance constrained optimization model to evaluate the economic and environmental impacts of biopower supply chains. Ann. Oper. Res. 296 (1–2), 95–130. http://dx.doi.org/10.1007/s10479-019-03331-x.

Khezerlou, H.S., Vahdani, B., Yazdani, M., 2021. Designing a resilient and reliable biomass-to-biofuel supply chain under risk pooling and congestion effects and fleet management. J. Clean. Prod. 281, 125101. http://dx.doi.org/10.1016/j.jclepro.2020.125101.

Kwon, O., Kim, J., J, Han., 2022. Organic waste derived biodiesel supply chain network: Deterministic multi-period planning model. Appl. Energy 305, 117847. http://dx.doi.org/10.1016/j.apenergy.2021.117847.

Lake, A., Acquaye, A., Genovese, A., Kumar, N., Koh, S.C.L., 2015. An application of hybrid life cycle assessment as a decision support framework for green supply chains. Int. J. Prod. Res. 53 (21), 6495–6521. http://dx.doi.org/10.1080/00207543.2014.951092.

Lo, S.L.Y., How, B.S., Teng, S.Y., Lam, H.L., Lim, C.H., Rhamdhani, M.A., Sunarso, J., 2021. Stochastic techno-economic evaluation model for biomass supply chain: A biomass gasification case study with supply chain uncertainties. Renew. Sust. Energ. Rev. 152, 111644. http://dx.doi.org/10.1016/j.rser.2021.111644.

Memisoğlu, G., Üster, H., 2021. Design of a biofuel supply network under stochastic and price-dependent biomass availability. IISE Trans. 53 (8), 869–882. http://dx.doi.org/10.1080/24725854.2020.1869870.

Mena, C., Schoenherr, T., 2020. The green contagion effect: an investigation into the propagation of environmental practices across multiple supply chains tiers. Int. J. Prod. Res. 1–18. http://dx.doi.org/10.1080/00207543.2020.1834160.

Miret, C., Chazara, P., Montastruc, L., Negny, S., Domenech, S., 2016. Design of bioethanol green supply chain: Comparison between first and second generation biomass concerning economic, environmental and social criteria. Comput. Chem. Eng. 85, 1635. http://dx.doi.org/10.1016/j.compchemeng.2015.10.008.

Mirhashemi, M.S., Mohseni, S., Hasanzadeh, M., Pishvaee, M.S., 2018. Moringa oleifera biomass-to-biodiesel supply chain design: An opportunity to combat desertification in Iran. J. Clean. Prod. 203, 313–327. http://dx.doi.org/10.1016/j.jclepro.2018.08.257.

Mittal, P., Kulkarni, K., Mitra, K., 2016. A novel hybrid optimization methodology to optimize the total number and placement of wind turbines. Renew. Energy 86, 133–147. http://dx.doi.org/10.1016/j.renene.2015.07.100.

Mohtashami, Z., Bozorgi-Amiri, A., Tavakkoli-Moghaddam, R., 2021. A two-stage multi-objective second generation biodiesel supply chain design considering social sustainability: A case study. Energy 233, 121020. http://dx.doi.org/10.1016/j.energy.2021.121020.

Nandimandalam, H., Aghalari, A., Gude, V.G., Marufuzzaman, M., 2022. Multi-objective optimization model for regional renewable biomass supported electricity generation in rural regions. Energy Convers. Manag. 266, 115833. http://dx.doi.org/10.1016/j.enconman.2022.115833.

Pantula, P.D., Mitra, K., 2020. Towards efficient robust optimization using data based optimal segmentation of uncertain space. Reliab. Eng. Syst. Saf. 197, 106821. http://dx.doi.org/10.1016/j.ress.2020.106821.

Rahmani Mokarrari, K., Aghamohamadi-Bosjin, S., Sowlati, T., Akhtari, S., Teja Malladi, K., Mirza, F., 2023. Techno-economic analysis of biofuel production from construction and demolition wood waste. Energy Sources Part B 18 (1), 2163723. http://dx.doi.org/10.1080/15567249.2022.2163723.

Razm, S., Dolgui, A., Hammami, R., Brahimi, N., Nickel, S., Sahebi, H., 2021. A two-phase sequential approach to design bioenergy supply chains under uncertainty and social concerns. Comput. Chem. Eng 145, 107131. http://dx.doi.org/10.1016/j.compchemeng.2020.107131.

Ruiz, J.A., Juárez, M.C., Morales, M.P., Muñoz, P., Mendívil, M.A., 2013. Biomass gasification for electricity generation: Review of current technology barriers. Renew. Sustain. Energy Rev. 18, 174–183. http://dx.doi.org/10.1016/j.rser.2012.10.021.

Saghaei, M., Ghaderi, H., Soleimani, H., 2020. Design and optimization of biomass electricity supply chain with uncertainty in material quality. Avail. Mark. Demand Energy 197, 117165. http://dx.doi.org/10.1016/j.energy.2020.117165.

Salehi, S., Mehrjerdi, Y.Z., Sadegheih, A., Hosseini-Nasab, H., 2022. Designing a resilient and sustainable biomass supply chain network through the optimization approach under uncertainty and the disruption. J. Clean. Prod. 359, 131741. http://dx.doi.org/10.1016/j.jclepro.2022.131741.

Sharma, S., Pantula, P.D., Miriyala, S.S., Mitra, K., 2021. A novel data-driven sampling strategy for optimizing industrial grinding operation under uncertainty using chance constrained programming. Powder Technol. 377, 913–923. http://dx.doi.org/10.1016/j.powtec.2020.09.024.

Simon, F., Girard, A., Krotki, M., Ordonez, J., 2021. Modelling and simulation of the wood biomass supply from the sustainable management of natural forests. J. Clean. Prod. 282, 124487. http://dx.doi.org/10.1016/j.jclepro.2020.124487.

Singh, S.K., Chauhan, A., Sarkar, B., 2022. Sustainable biodiesel supply chain model based on waste animal fat with subsidy and advertisement. J. Clean. Prod. 134806. http://dx.doi.org/10.1016/j.jclepro.2022.134806.

Singh, V.K., Singal, S.K., 2017. Operation of hydro power plants-a review. Renew. Sustain. Energy Rev. 69, 610–619. http://dx.doi.org/10.1016/j.rser.2016.11.169.

Smith, L., Ibn-Mohammed, T., Koh, S.L., Reaney, I.M., 2018. Life cycle assessment and environmental profile evaluations of high volumetric efficiency capacitors. Appl. Energy 220, 496–513. http://dx.doi.org/10.1016/j.apenergy.2018.03.067.

Sun, O., Fan, N., 2020. A review on optimization methods for biomass supply chain: models and algorithms, sustainable issues, and challenges and opportunities. Proc. Integr. Optim. 4 (3), 203–226. http://dx.doi.org/10.1007/s41660-020-00108-9.

Tesfamichael, B., Montastruc, L., Negny, S., Yimam, A., 2021. Designing and planning of Ethiopia's biomass-to-biofuel supply chain through integrated strategic-tactical optimization model considering economic dimension. Comput. Chem. Eng. 153, 107425. http://dx.doi.org/10.1016/j.compchemeng.2021.107425.

Tillman, D.A., 2000. Biomass cofiring: the technology, the experience, the combustion consequences. Biomass Bioenergy 19 (6), 365–384. http://dx.doi.org/10.1016/S0961-9534(00)00049-0.

Tordecilla, R.D., Juan, A.A., Montoya-Torres, J.R., Quintero-Araujo, C.L., Panadero, J., 2021. Simulation–optimization methods for designing and assessing resilient supply chain networks under uncertainty scenarios: A review. Simul. Model. Pract. Th 106, 102166. http://dx.doi.org/10.1016/j.simpat.2020.102166.

Wolff, M., Becker, T., Walther, G., 2023. Long-term design and analysis of renewable fuel supply chains-an integrated approach considering seasonal resource availability. Eur. J. Oper. Res 304 (2), 745–762. http://dx.doi.org/10.1016/j.ejor.2022.04.001.

Wu, J., Zhang, J., Yi, W., Cai, H., Li, Y., Su, Z., 2022. Agri-biomass supply chain optimization in north China: Model development and application. Energy 239, 122374. http://dx.doi.org/10.1016/j.energy.2021.122374.

Yang, L., Wang, Y., Wang, R., Klemeš, .J.J., Almeida, C.M.V.B.D., Jin, M., Zheng, X., Qiao, Y., 2020. Environmental-social-economic footprints of consumption and trade in the Asia-Pacific region. Nat. Commun. 11 (1), 1–9. http://dx.doi.org/10.1038/s41467-020-18338-3.

Zandi Atashbar, N., Labadie, N., Prins, C., 2018. Modelling and optimisation of biomass supply chains: a review. Int. J. Prod. Res. 10, 3482–3506. http://dx.doi.org/10.1080/00207543.2017.1343506.